HERON is jointly edited by:
STEVIN-LABORATORY of the department of Civil Engineering, Delft University of Technology, Delft, The Netherlands
and
INSTITUTE TNO for Building Materials and Building Structures. Rijswijk (ZH), The Netherlands.
HERON contains contributions based mainly on research work performed in these laboratories on strength of materials, structures and materials science.

Secretary:
G. J. van Alphen
Stevinweg 1
P.O. Box 5048
2600 GA Delft, The Netherlands
Tel. 0031-15-785919
Telex 38070 BITHD

HERON vol. 29 1984 no. 4

Contents

FATIGUE FAILURE OF CONCRETE IN TENSION

H. A. W. Cornelissen
Delft University of Technology
Department of Civil Engineering
Stevin Laboratory
Stevinweg 4, P.O. Box 5048, 2600 GA Delft, The Netherlands

CUR VB

This publication has been issued in close co-operation with the Netherlands Committee for Research, Codes and Specifications for Concrete (CUR-VB).

Publications in HERON since 1970

Abstract

Concentric tensile and flexural tensile fatigue tests were carried out on plain concrete specimens. The effects of pulsating tensile loadings as well as of alternating tensile-compressive loadings were studied. The results of the constant-amplitude tests have been presented in S-N diagrams and a Goodman diagram.

From these results it emerged that fatigue life was strongly reduced by alternation of the stress from tension to compression. Furthermore the number of cycles to failure for wet specimens was lower than for dry ones. It was also found that for equal load signals applied, flexural tests resulted in longer fatigue lifes than concentric tests, probably because of the possibility of redistribution of stresses.

The longitudinal strains of the concentric tests were analysed. This resulted in a strong relation between strain rate and fatigue life. The concentric tests were continued with program-loading tests in order to check Miner's rule.

Based on strain rate Miner's rule could be verified and Miner's number, $M = 1$, at failure turned out to be safe in general.

Key words

Concrete, tension, flexure, fatigue, stress reversals, tensile strain, strain rate, Miner's rule, testing methods.

FATIGUE FAILURE OF CONCRETE IN TENSION

Foreword

The effect of repeated tensile and alternating tensile-compressive stresses on the fatigue behaviour of plain concrete is the subject of this Heron issue. The research project was carried out with the supervision of CUR-VB Committee C-33, which was constitued as follows:

Ir. W. Colenbrander, Chairman
Ir. P. Eggermont, Secretary
Ir. J. P. Coppin
Dr. Ir. H. A. W. Cornelissen
Ir. F. F. M. de Graaf
Ir. B. Kuiper
Prof. Ir. H. Lambotte
Ir. J. van Leeuwen
Ir. B. J. G. van der Pot
Ir. A. J. M. Siemes
Ir. Drs. J. H. A. M. Vrencken
Ir. H. P. J. Vereijken, CUR-VB
Ir. W. Stevelink, Mentor

Ir. H. A. Körmeling and Ir. D. Zijp left the Committee in 1981 and Ir. P. H. Zaalberg in 1984.

The research was carried out by Dr. Ir. H. A. W. Cornelissen in the Stevin Laboratory of the Delft University of Technology and by Ir. M. Jacobs in the Magnel Laboratory of the State University of Ghent (Belgium), who also was author of the chapters 2.2.2, 3.3 and 4.2.2.

Financial support was provided by CUR-VB, MaTS, Delft University of Technology, State University of Ghent and Belgian Ministry of Public Works.

The present issue of Heron is mainly based on CUR-VB/MaTS-IRO report No. 116 entitled "Fatigue of concrete. Part 2: tensile and tensile-compressive stresses". The results presented in report No. 116 have been completed with results of program-loading tests as described in chapter 5 of the present issue.

Because most diagrams of this Heron issue have been published in CUR-VB/MaTS-IRO report No. 116, the captions are in English as well as in Dutch.

Fatigue failure of concrete in tension

1 Introduction

This report - "Fatigue failure of concrete in tension" - deals with the influence of pulsating tensile loads and of alternating tensile-compressive loads. It has been prepared by CUR-VB Committee C 33 "Alternating load", as was also a report on fatigue of concrete in compression [1]. This Committee was set up because available knowledge concerning the fatigue behaviour of concrete was considered inadequate, while it is important in connection with offshore structures, among others.

Indeed, fatigue may play a part wherever stresses fluctuate with time. In this context the effect of waves, wind, current and live load due to traffic must be considered, but also the effect of, for example, temperature variations on the stresses in structures. In such situations failure of the material may occur at stresses below its static strength.

The resistance of concrete to tensile stress is about 10 to 20 times less than its resistance to compressive stress. As the tensile strength moreover exhibits considerable scatter, it is often neglected in the design of concrete structures. Also, in certain cases (e.g., fully prestressed concrete) the designer may try to ensure that no tensile stresses will occur in the concrete.

This might suggest that the behaviour of concrete subjected to tensile stresses is not relevant. However, as a result of the application of limited and of partial prestressing, in which some tensile stress is allowed in the concrete, interest in the behaviour of concrete in tension is increasing.

The tensile strength governs the cracking behaviour and therefore also, among other characteristics, the stiffness, the damping action, the bond to embedded steel, and the durability of concrete. The tensile strength is also of importance with regard to the behaviour of concrete in shear. Besides, it constitutes a component in modelling the multiaxial behaviour of concrete. And information on how concrete responds to tensile stresses is needed more particularly also in connection with the increasing importance and application of modern structural safety considerations.

So far as experimental research was concerned, Committee C 33 had input from three laboratories, namely: TNO-IBBC (TNO Institute for Building Materials and Building Structures), the Stevin Laboratory of the Delft University of Technology (THD), and the Magnel Laboratory of the State University of Ghent (RUG) in Belgium. The abovementioned investigation of the fatigue of concrete in compression was carried out by TNO-IBBC. The other two laboratories concentrated on the effect of tensile and of tensile-compressive loads on fatigue behaviour. For this purpose THD carried out concentric uniaxial tests and RUG carried out three-point bending tests. The bending tests were financed jointly by RUG and the Belgian Ministry of Public Works. The cost of the other research was met in part by the institutes concerned, im part by CUR-VB (Nether-

lands Committee for Research, Codes and Specifications for Concrete) and later also by MaTS (Marine Technological Research).

This report describes constant-amplitude tests and deals also with program loading tests performed in verification of Miner's rule for concrete loaded in tension.

2 The present position

2.1 *General*

Fatigue tests in which the stresses pulsate within the tensile range or in which they alternate between tension and compression can be performed in various ways. Because they are relatively simple to carry out, tests on specimens loaded in bending or on specimens subjected to splitting load are often preferred for the purpose. Alternating tensile-compressive stresses are obtained by means of prestress applied to bending test specimens or by means of lateral compressive force in the case of splitting tests (see Figs. 1a and 1b).

Tests in direct (concentric or axial) tension are also performed. To ensure that the load acts concentrically on the specimen, special gripping jaws are needed, often in combination with an appropriately adapted shape of the specimen. With the advent of modern epoxy glues the problem of correctly applying the tensile load has become simpler, however. Besides, it is thus possible to apply a tensile load to the same face as a compressive load, so that in principle concentric uniaxial alternating tensile-compressive tests can be performed (see Fig. 1c).

Before reviewing the relevant literature giving results of fatigue tests, the above-mentioned three testing methods will be briefly discussed and compared because it appears that the results obtained are influenced by the method employed.

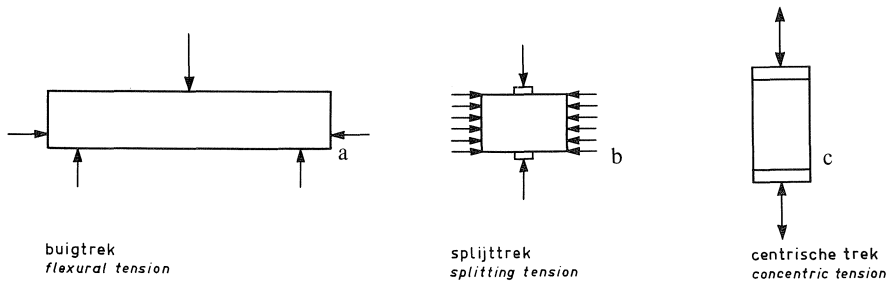

Fig. 1. Some test methods for producing pulsating tensile or alternating tensile-compressive stresses.

Concentric tensile test

In a test under direct tension the uniaxial load is applied concentrically to the specimen. Apart from effects due to the heterogeneous character of concrete, there is an equal and uniform stress distribution at every section.

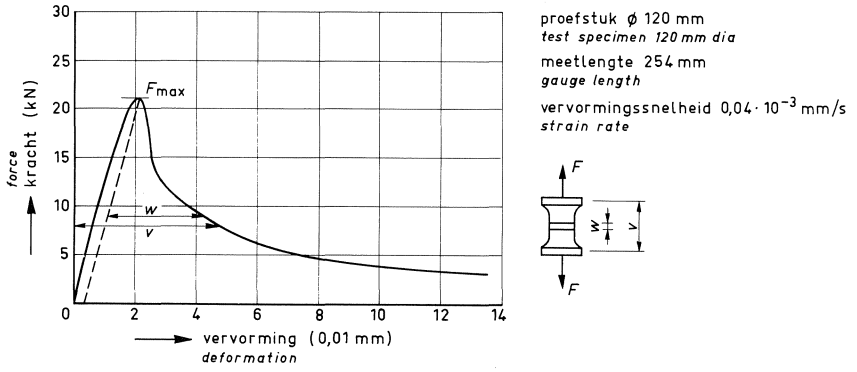

Fig. 2. Force-deformation diagram of a strain-controlled tensile test.

A load-controlled tensile test is often used for determining the stress-strain diagram. In such a test the applied load increases at a constant rate per unit time. Failure of the specimen occurs when, as a result of cracking and crack propagation, it can no longer resist the force acting upon it as that point of time.

This type of test yields no information on the forces that can still be transmitted after the concrete has cracked. Such information can, however, be obtained from a deformation-controlled test in which the rate at which the deformation of the specimen increases per unit time is constant. When the force that the specimen can transmit decreases as the cracks become larger, the applied load must be reduced. This has to be done promptly, which imposes special requirements on the test apparatus.

Fig. 2 shows a force-deformation diagram as obtained in a deformation-controlled (or strain-controlled) tensile test. It appears from this diagram that when v increases, F increases to F_{max}. Thereafter, with further increase of v, F decreases. In the last-mentioned situation the deformation v is composed of two components, namely: the width of crack zone w and deformation in the regions outside this zone. As the diagram shows, forces can still be transmitted even at deformations which are many times larger than the deformation associated with F_{max}. This information is not obtainable from a load-controlled test: in such a test only the part situated to the left of the deformation associated with F_{max} can be recorded.

Bending test

A bending (or flexural) test is usually performed as a three-point or a four-point test. In the latter the load is divided between two points of application, the bending moment being constant between these points. In order to determine the stress distribution at a section in a bending test it is necessary to make assumptions as to the relation between stress and strain. It is not a linear relation, especially at higher values of the stress. Because of this the stress is usually not accurately known, which is a drawback of this testing method. As in a direct (concentric) tensile test, a bending test can be load-controlled or deformation-controlled.

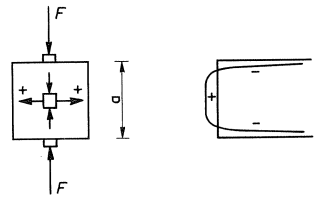

Fig. 3. Stress distribution in a splitting test.

Splitting test

Another indirect method of producing tensile stress in a specimen is the so-called Brazilian splitting test. A horizontal tensile stress is generated by means of a vertical compressive load F (see Fig. 3). For a cube specimen this stress can be approximately calculated from:

$$\sigma_b = \frac{2F}{\pi a^2} \tag{1}$$

An important difference between the three above-mentioned methods of testing is that in the concentric tensile test the same maximum stress exists in every section of the specimen, whereas in the four-point bending test this is the case only in the region where the bending moment is constant. In the three-point bending test and the splitting test the maximum stress occurs at just one section. Besides, in the splitting test the loading condition is biaxial.

The (tensile) strength of the concrete in the test specimen is not constant in that it varies from one region to another, some of which will constitute "weak links", as it were. In a concentric tensile test the weakest link will always be loaded to its maximum capacity, so that failure will occur there. In a four-point bending test there is less likelihood that the weakest link will be located in the constant (maximum) bending moment zone, and in a three-point bending test or a splitting test there is indeed considerable probability that the weakest link will not be located at the section where the highest stresses occur. In such cases higher "apparent" strengths will therefore be found.

This effect, coupled with the fact that assumptions have to be made as to the stress distribution that occurs, explains why different tensile strength values are obtained from the above-mentioned respective testing methods. A linear relation between stress and strain is often assumed.

Thus, for example, it is found that the flexural (tensile) strength obtained in the four-point bending test is approximately twice, and the splitting (tensile) strength about 1,5 times, as high as the direct tensile strength [2]. These ratios are more particularly found to depend on the absolute magnitude of the strength.

Another distinction exists in that there is a uniform stress distribution in a concentric tensile test. In the other testing methods there is a stress gradient, which influences the magnitude of the tensile strength. This has been demonstrated by, for example, Heilmann [3] who performed, among others, eccentric deformation-controlled tensile tests

on concrete. From his research it emerges that with increasing eccentricity of the load (steeper gradient) the ultimate strain of the test specimen becomes larger, as does the maximum stress that can be resisted. These results are obtained from measurements carried out on the most deformed face of the specimen.

From what has been said above it follows that in the interpretation of the results it is necessary to take account of how they were obtained and of the fact that they are not directly applicable to situations other than those investigated.

2.2 *Review of the literature*

2.2.1 Concentric tension

Fatigue tests in which concrete is loaded in direct (concentric) tension have, partly because of the difficult testing procedure, been carried out only on a very limited scale.

Two researches on the subject have been reported in the literature [4, 5]. Constant-amplitude tests (15 Hz) on concrete mixes destined for highway engineering are described in [4]. In those tests a low cement content was used, approximately 115 kg/m^3. The lower stress limit was always a little above zero in order to ensure proper clamping of the specimens. The upper stress limit was referred to the static tensile strength. A coarse and a fine grading (granulometric composition) of the mix was employed in the tests. In both cases the maximum particle diameter was 18 mm.

The results of the tests are presented in Fig. 4, in which the results reported in [5] have also been included. In the latter case the specimens, consisting of mortar, were tested at a frequency of 10 Hz. Lower fatigue life values were obtained in these tests, this being due to the more brittle behaviour of mortar as compared with that of concrete. This is also one of the reasons why the more finely graded mix in [4] attained a lower number of cycles to failure than did the mix with coarser grading.

So far as is known, no results of concentric tests with load varying between tension and compression have been published.

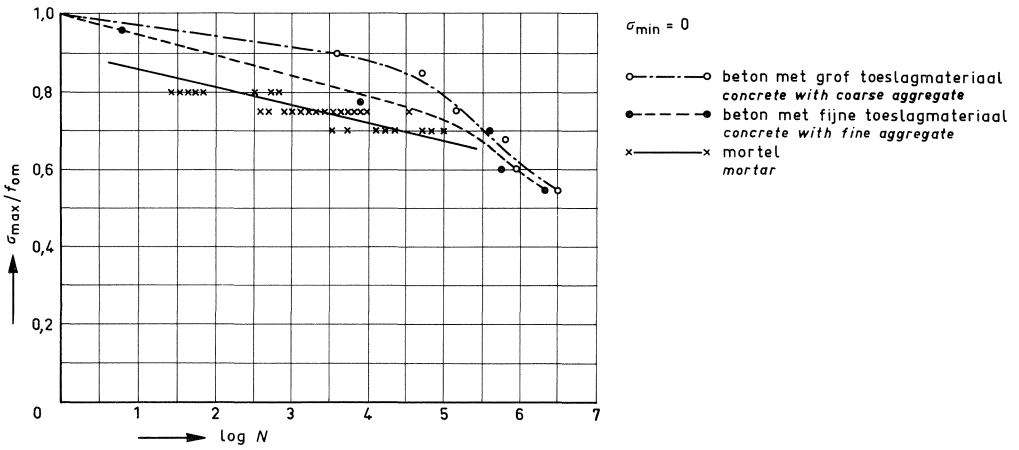

Fig. 4. S-N curves for concrete.

2.2.2 Flexural tension

The information published in the literature is concerned mainly with the fatigue behaviour of plain concrete subjected to flexural tensile load. On the other hand, only a small number of research results relating to alternating flexural tensile-compressive load have been reported.

The investigations can thus be divided into two general types:

- tests in which a bending moment acts in one direction only (the bottom extreme fibre of the test specimen is subjected to varying tensile stress only: pulsating stress);
- tests in which a bending moment acts alternately in one direction and then in the other (the bottom extreme fibre is subjected to alternating tensile and compressive stress).

Flexural tests of the first-mentioned type are exemplified by Raithby's experiments [6]. He performed four-point bending tests on plain concrete prisms with dimensions of 102 mm × 102 mm × 508 mm. Three different mixes were used, with cube strengths ranging from 21 to 45 N/mm^2 and flexural strengths from 2,0 to 3,5 N/mm^2. All the specimens were stored under water and were tested at various ages (from 4 weeks to 5 years), the loading frequency being 20 Hz.

If the maximum stress in the bottom extreme fibre is expressed as a percentage of the static flexural strength f_c associated with the age of testing, the results can be represented by one S-N curve (see Fig. 5).

Experimental results of compressive tests are analysed by Hsu in [7]. For this purpose the influence of the frequency is introduced with the aid of the stress-time diagram given by Rüsch [8]. Two equations are established with which the fatigue behaviour of concrete can be predicted. These equations are found to be valid also for bending:

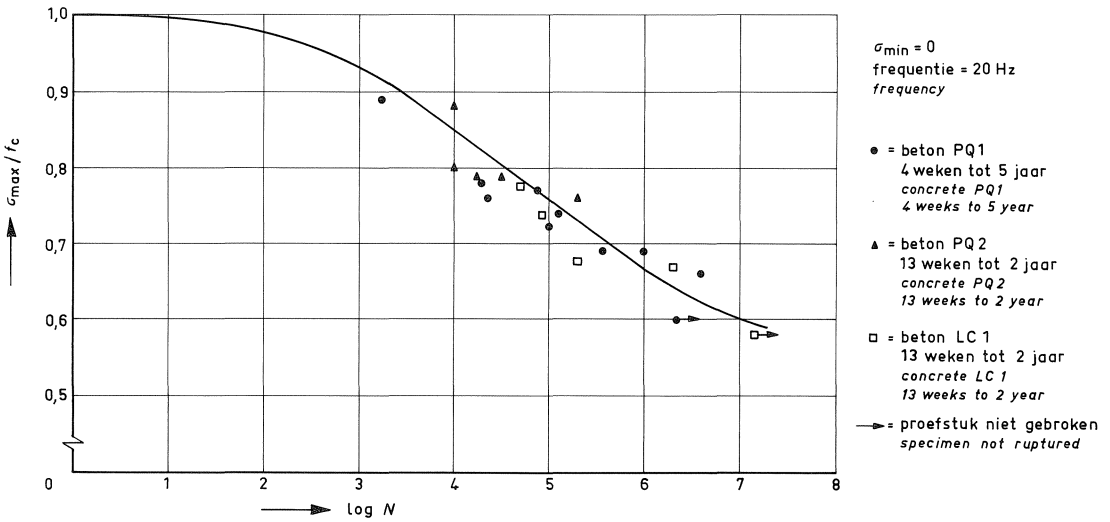

Fig. 5. S-N curve for concrete subjected to flexural tensile cycles, according to RAITHBY [6].

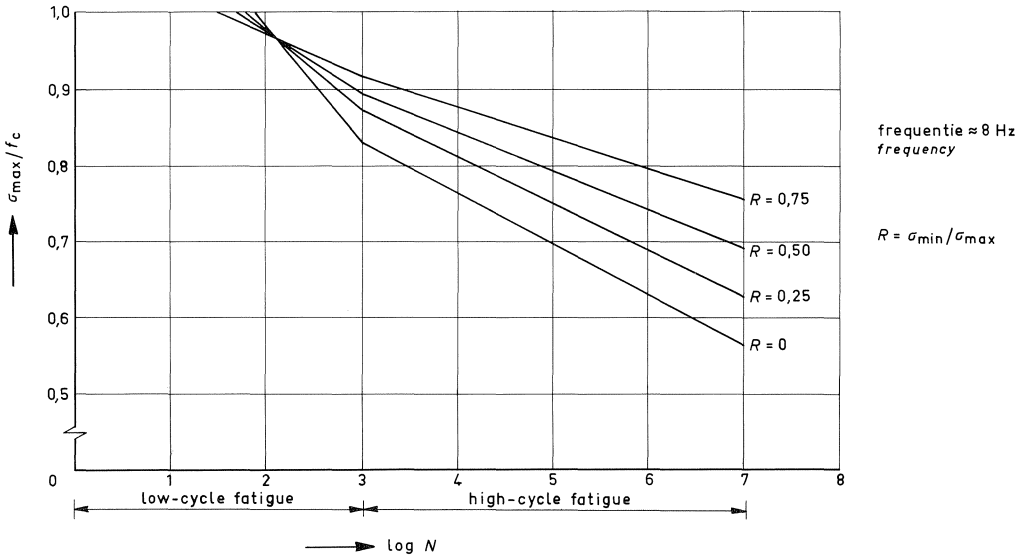

Fig. 6. S-N curves for concrete subjected to flexural tensile cycles, according to Hsu [7].

for $N < 10^3$:

$$\frac{\sigma_{max}}{f_c} = 1{,}20 - 0{,}20R - 0{,}133(1 - 0{,}779R) \log N - 0{,}053(1 - 0{,}445R) \log T \quad (2)$$

for $10^3 < N < 10^7$:

$$\frac{\sigma_{max}}{f_c} = 1 - 0{,}0662(1 - 0{,}556R) \log N - 0{,}0294 \log T \quad (3)$$

Since the period T determines the loading rate and the product $N \times T$ represents the duration of loading, the equations (2) and (3), in which σ_{max} = function (N, R, T), simultaneously take account of the effect of loading duration and rate. By way of example these two equations are represent in Fig. 6 for the special case where $T = 0{,}120$ s (frequency approx. 8 Hz) and for various values of the parameter R.

Bending tests of the second type, in which the bottom fibre stress varies between a tensile stress σ_{max} and a compressive stress σ_{min} of equal absolute magnitude have, so far as is known, been carried out only by Hatt and Crepps [9, 10], Williams [11] and McCall [12].

In the literature such experiments are referred to as "completely reversed flexural loading".

Hatt and Crepps tested prismatic specimens (102 mm × 102 mm × 762 mm), fixed at one end and subjected to an alternating moment at the other (free) end. A low frequency of loading (0,166 Hz) was applied in order to simulate traffic loads on a road.

Their results are given in Fig. 7. It appears that concrete has a fatigue limit in the tension-compression range which is equal to 55% of the static flexural (tensile) strength.

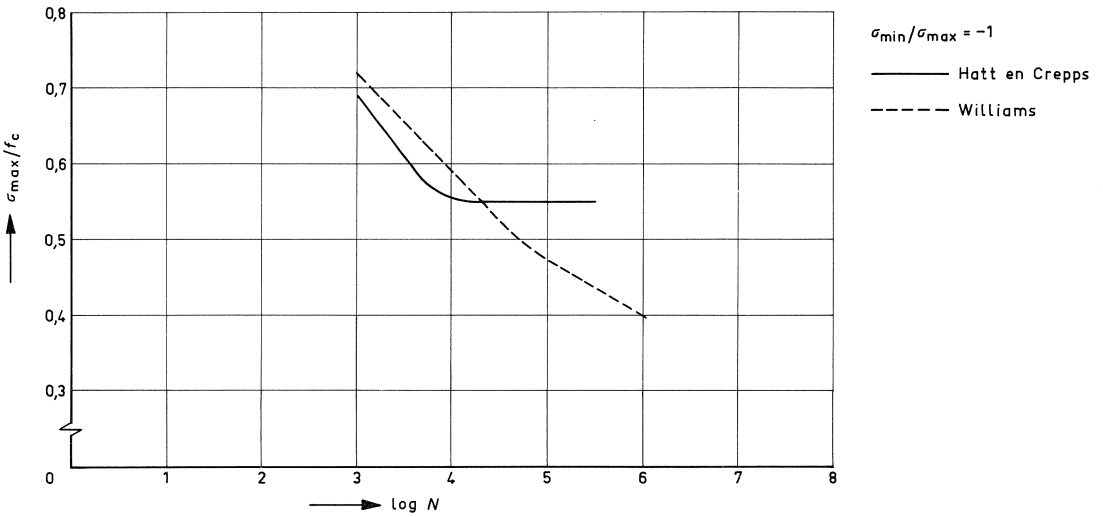

Fig. 7. S-N curves for concrete subjected to alternating flexural tension and compression ("reversed bending").

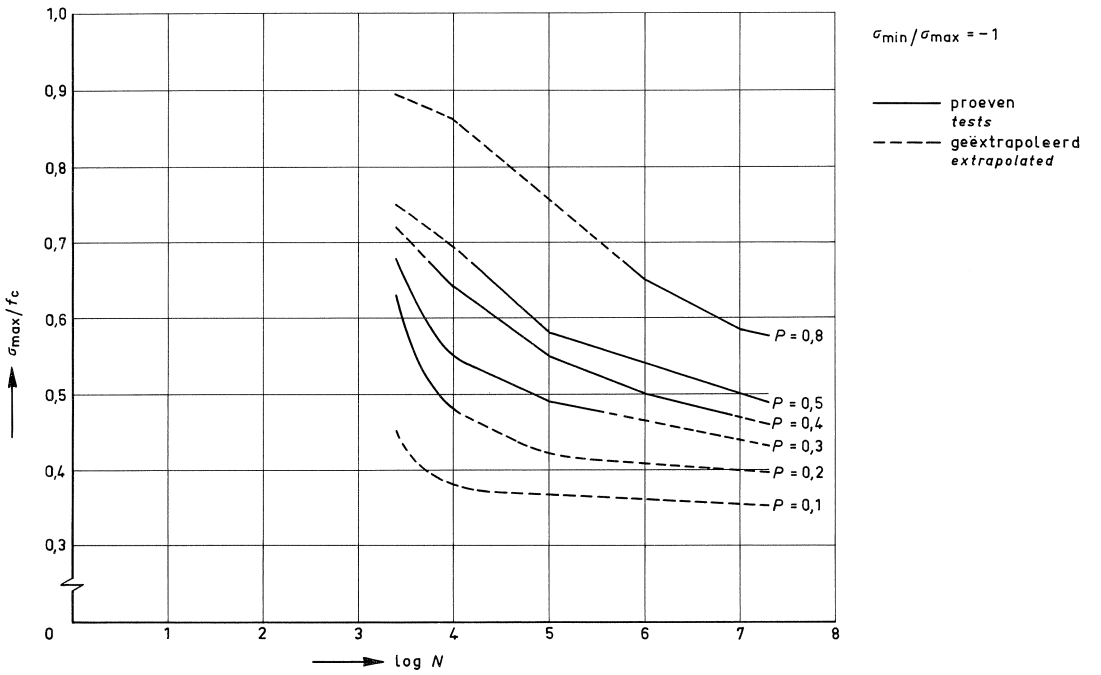

Fig. 8. S-N curves for concrete subjected to alternating flexural tension and compression, for different values of failure probability P, according to McCall [12].

Williams carried out fatigue tests on lightweight concrete with a compressive strength of 21 N/mm^2 and a flexural strength of 2,7 N/mm^2. The specimens (102 mm × 130 mm × 826 mm) were loaded alternately in bending with a frequency of 0,25 Hz. The results (Fig. 7) show that the fatigue strength at 10^6 load cycles is equal to 40% of the static flexural strength. As contrasted with the findings of Hatt and Crepps, no fatigue limit was found in these tests.

McCall reports the results of fatigue tests on small concrete beams (76 mm × 76 mm × 368 mm) subjected to up to 2×10^7 load cycles at a frequency of 30 Hz. The maximum stress in these tests was varied between 47,5% and 67,5% of the static strength, and 20 tests were performed for each stress level. In Fig. 8 the results are represented by S-N curves for various values of $P\{\text{failure}\}$ (i.e., the probability that failure will occur at a number of load cycles smaller than, or equal to, the number of cycles producing failure). It appears from the diagram that even at 2×10^7 cycles of the applied stress there was no ascertainable fatigue limit. At 2×10^7 cycles the fatigue strength is 49% of the static tensile strength for $P\{\text{failure}\} = 0{,}5$ and is 58% for $P\{\text{failure}\} = 0{,}8$.

Having regard to the stochastic character of the fatigue phenomenon, McCall's research has made a notable contribution to the statistical analysis of the results of such tests.

2.2.3 Splitting tension

The fatigue behaviour of concrete under repeated tensile loading has also been investigated with the aid of splitting tests.

For this purpose Linger and Gillespie [13] used cylindrical specimens (75 mm diameter × 150 mm) with an average compressive strength of 23 N/mm^2. For the fatigue tests (at 9 Hz) the upper stress limit was referred to the static splitting tensile strength. The lower limit was always zero. The results are represented in Fig. 9.

This diagram also includes the results of fatigue tests under concentric compression performed on similar cylinders. In these tests the stress level was referred to the cylin-

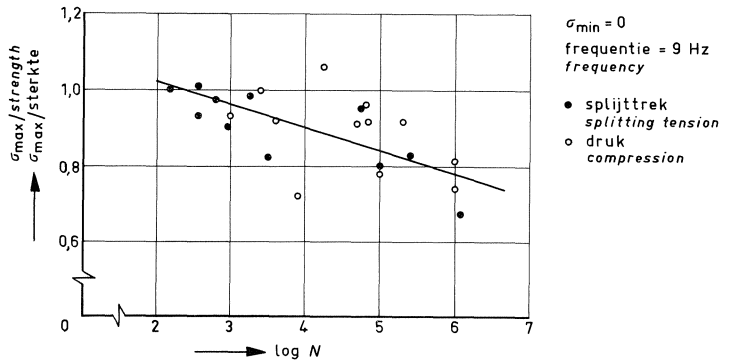

Fig. 9. S-N curve for splitting tensile and for compressive stress cycles, according to LINGER and GILLESPIE [13].

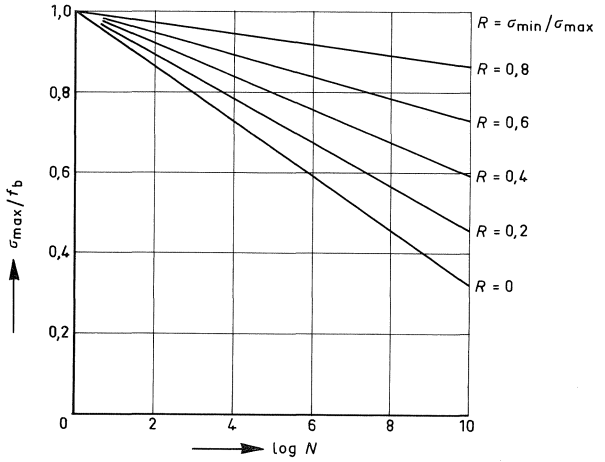

Fig. 10. S-N curves according to TEPFERS [14]

der (compressive) strength. As shown here, the number of cycles to failure was approximately the same in both cases. This leads those authors to the conclusion that tensile fatigue and compressive fatigue are governed by the same material property.

Tepfers [14] also reports that, if the stresses are referred to the tensile and to the compressive strength respectively, the number of cycles to failure in tension is equal to that in compression. This is expressed by the formula:

$$\frac{\sigma_{max}}{f'_c} = 1 - \beta \left(1 - \frac{\sigma_{min}}{\sigma_{max}}\right) \log N \tag{4}$$

The average value of β for tension is found to be the same as that for compression, namely: $\beta = 0{,}0685$.

The tests performed by Tepfers were compressive and splitting tests on 150 mm cubes, at a frequency of 10 Hz. A number of S-N curves calculated with the aid of formula (4) are given in Fig. 10.

He also performed splitting tests in which the specimens were subjected to a uniformly distributed constant compressive preload in a direction perpendicular to that of the splitting load [15]. In this way it was possible to apply alternating tensile and compressive stress (see Fig. 11).

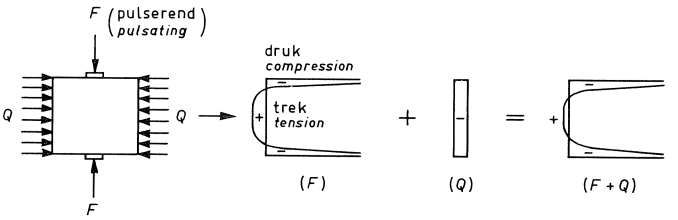

Fig. 11. Stress distribution due to a splitting load F and a lateral compressive load Q.

In these tests the lower limit was, respectively, 53% and 63% of the compressive strength and the upper limit was 65% of the splitting tensile strength.

It was inferred from the tests that cycles alternating between tension and compression result in virtually the same life as is attained in a situation where the stress pulsates between zero and a limit value equal to the relative compressive or tensile stress (depending on which is the greater). For example, in a case where the stress varies between 30% of the compressive strength and 70% of the tensile strength, it is considered that the fatigue life attained (the number of cycles endured) is the same as when the stress pulsates between zero and 70% of the tensile strength.

As it proved difficult correctly to produce the relatively small stresses in the tensile range, the above conclusion must be viewed with some caution.

3 Constant-amplitude tests

3.1 *Aims and scope of the tests*

As there was only a limited amount of relevant information available in the literature, Committee C 33 decided to carry out its own research. The tests chosen for the purpose were of two kinds: uniaxial concentric tensile tests (direct tension) and flexural tests in which the bottom fibre was subjected to pulsating tensile stress or, with the aid of a prestress, to alternating tensile and compressive stress.

The concentric tensile tests were performed in the Stevin Laboratory of the Delft University of Technology (THD), and the flexural tests were performed in the Magnel Laboratory of the State University of Ghent (RUG) in Belgium.

The advantage of the flexural tests is that they tie up well with loading conditions as encountered in actual practice. Against this there is the drawback that the stress distribution at the cross-section is - partly on account of non-linear behaviour - not sufficiently accurately known, which is a complication in seeking to generalize the test results.

Concentric tensile tests do not suffer from this disadvantage and are therefore more suitable for investigating the phenomenon of fatigue of concrete. In order to enable the results of the two investigations to be compared with one another, a number of experimental conditions such as concrete mix composition and age at testing were co-ordinated.

The object of the experimental research was, primarily, to determine the number of cycles to failure for various combinations of lower and upper limit of the pulsating or the alternating stress. In the concentric tensile tests the longitudinal deformations were also recorded, which were then co-ordinated with cracking and crack propagation in the specimen during fatigue.

The constant-amplitude tests were characterized by sinusoidal cyclic variations with a frequency of 6 Hz (THD) and 8 Hz (RUG). The number of cycles was limited to a maximum of 2×10^6. Specimens which had not failed on reaching this maximum were designated as "run-outs".

The upper limit (σ_{max}) and the lower limit (σ_{min}) of the alternating or the pulsating stress were determined as percentages of the static tensile strength (concentric, i.e., direct, tensile strength for THD; flexural strength, i.e., modulus of rupture, for RUG) and of the static compressive strength of the concrete.

The stress combinations employed in the THD and RUG tests are summarized in Table 1.

Table 1. Review of the tests performed at Delft (concentric tension) and at Ghent (flexural tension)

upper limit	lower limit								
tension σ_{max}/f_{om} or σ_{max}/f_c	tension σ_{min}/f_{om} (or f_c)				compression σ_{min}/f'_{cm}				
	0,40	0,30	0,20	0,00	0,05	0,10	0,15	0,20	0,30
0,40					D	D	D	D,G	D,G
0,45									
0,50					D	D,G		D,G	D,G
0,55									
0,60	D	D	D	D,G	D	D,G	D	D,G	D,G
0,65	D	D	D	D					
0,70	D	D	D	D,G	D	D,G	D	D,G	D,G
0,75	D	D	D	D					
0,80	D	D	D	D,G	D	D,G	D	D,G	D,G
0,85	D	D	D	D					
0,90	D	D	D	D,G	D	D,G	D	D,G	D,G

D = tests at Delft (THD)
G = tests at Ghent (RUG)

3.2 *Concentric tension and concentric tension-compression*

3.2.1 General

Tests were performed in which the load varied between predetermind limits (see Fig. 12). The upper limit was chosen in the range from 40% to 90% of the static tensile strength, while the lower limit was 0, 20, 30 or 40% of the static tensile strength. In order to investigate the effect of a compressive stress on the fatigue behaviour under tension, tests were moreover performed in which the lower limit was 10, 20 or 30% of the static compressive strength. With these relatively low compressive stresses it could be presumed that they would not given rise to compressive failure.

In the second part of the research only a testing machine with a maximum capacity of 100 kN was available. For this reason values of 5% and 15% of the static compressive strength were adopted for the lower stress limit in these tests.

The tests were carried out with specimens which were stored in water for 2 weeks after casting and were then kept in the laboratory (i.e., in full contact with the air) for a further 2 weeks. Besides these "dry" specimens, "wet" specimens were also used in the research. These were obtained by sealing the specimens in plastic film, thus enabling

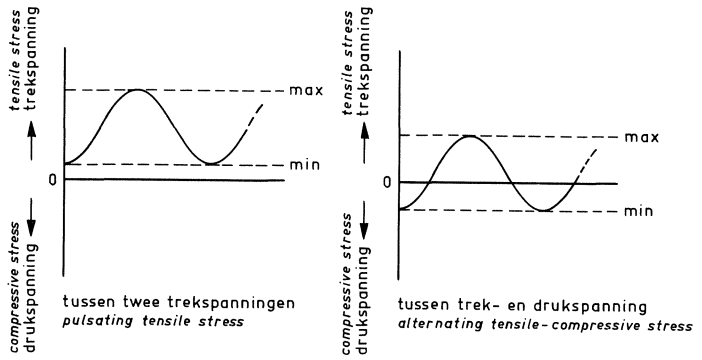

Fig. 12. Stress variation ranges.

the effect of the moisture condition also to be investigated. Besides, with the wet specimens the deformations were not affected by shrinkage. Deformation measurements were carried out with a view to correlating them with internal cracking that occurred as fatigue developed. Also, a theoretical model was established for this behaviour.

3.2.2 Test procedure

The test specimens were cylinders 300 mm in length and with a least diameter of 120 mm (see Fig. 13). In the main, one concrete mix was used, as specified in Table 2. The average cube strength of the concrete investigated was 47,3 N/mm^2 ($V(f_c') = 3{,}8\%$). In the dynamic tests the limits between which the stress varied were referred to the static compressive and tensile strengths. Accordingly, these strengths were determined for each batch of concrete used. Out of a batch comprising 12 cylinders and six cubes (150 mm size) always three cubes were used for determining the compressive strength,

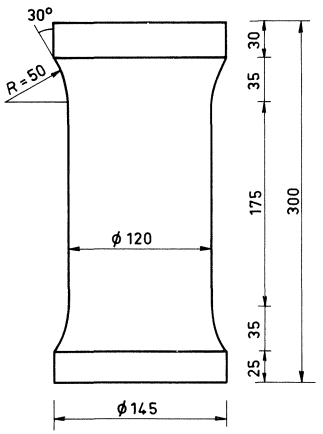

Fig. 13. Shape and dimensions of the specimen for the concentric tensile tests.

Table 2. Concrete mix composition for the concentric tensile tests

type of cement	portland cement class B
cement content	325 kg/m^3
aggregate (gravel + sand)	1942 kg/m^3
water-cement ratio	0,50
maximum particle diameter	16 mm

three cubes for determining the splitting strength and five or six cylinders for determining the concentric tensile strength.

In the static compressive tests the loading rate was 0,47 N/mm^2 · s and in the tensile tests it was 0,1 N/mm^2 · s.

The average concentric tensile strength was 2,46 N/mm^2 ($V(f_0) = 7{,}6\%$) for the dry specimens. For these specimens Fig. 14 shows the range within which 95% of the measured stress-strain curves are situated. The ultimate strain was found to be 0,01% on average. An average tensile strength of 2,92 N/mm^2 ($V(f_0) = 3{,}7\%$) was obtained for the wet specimens.

Table 3 gives the average results obtained in the static tests. Appendix A contains an overview of all the results. It is to be noted that the modulus of elasticity (secant modulus) was determined at 40% of the tensile strength and that the ultimate strain ε_1 was measured at the maximum tensile stress. Fig. 15 shows a specimen of the kind used for the static (and fatigue) tests.

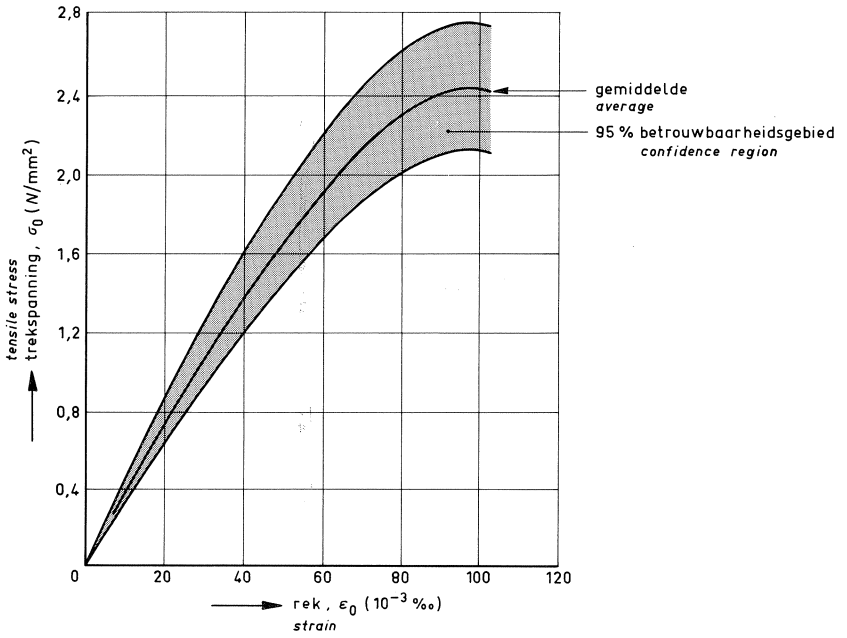

Fig. 14. Stress-strain diagram for dry concrete subjected to concentric tensile loading.

Table 3. Average values from the static tests (THD)

	compression	splitting tension		concentric tension		
	f'_{cm} (N/mm^2)	f_{bm} (N/mm^2)		f_{om} (N/mm^2)	E_{bm} (N/mm^2)	ε_{1m} (10^{-6})
average	47,34	2,87	dry	2,46	36140	96
			wet	2,92	35515	125
coefficient	3,8%	7,0%	dry	7,6%	5,2%	9,6%
of variation			wet	3,7%	5,6%	7,7%

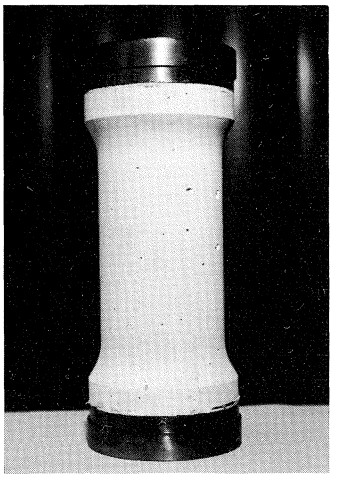

Fig. 15. Concentric tensile test specimen.

The static tensile tests and also the fatigue tests were performed on a machine of 100 kN capacity. A machine of higher capacity was used only for the fatigue tests in which the lower limit was 30% of the compressive strength.

In order to apply the load axially (concentrically) to the specimen, the latter was mounted between swivel heads. These had to be prestressed so as to achieve freedom from slack or play at zero load in the tests with alternating tension and compression. Fig. 16 is a general view of the test set-up. Steel plates were bonded to the upper and the lower face in order to transmit the tensile load to the specimen. A press was used for bonding the plates, thus ensuring that they were axially positioned and plane-parallel. The longitudinal deformation was measured with inductive displacement transducers in two positions located on opposite faces.

A microcomputer was constructed for generating the load signal and recording the measured data. The signal generated for the tests is shown in Fig. 17. It shows that the dynamic load was applied gradually in such a way that the predetermined upper and lower limits of the load were attained after about six cycles.

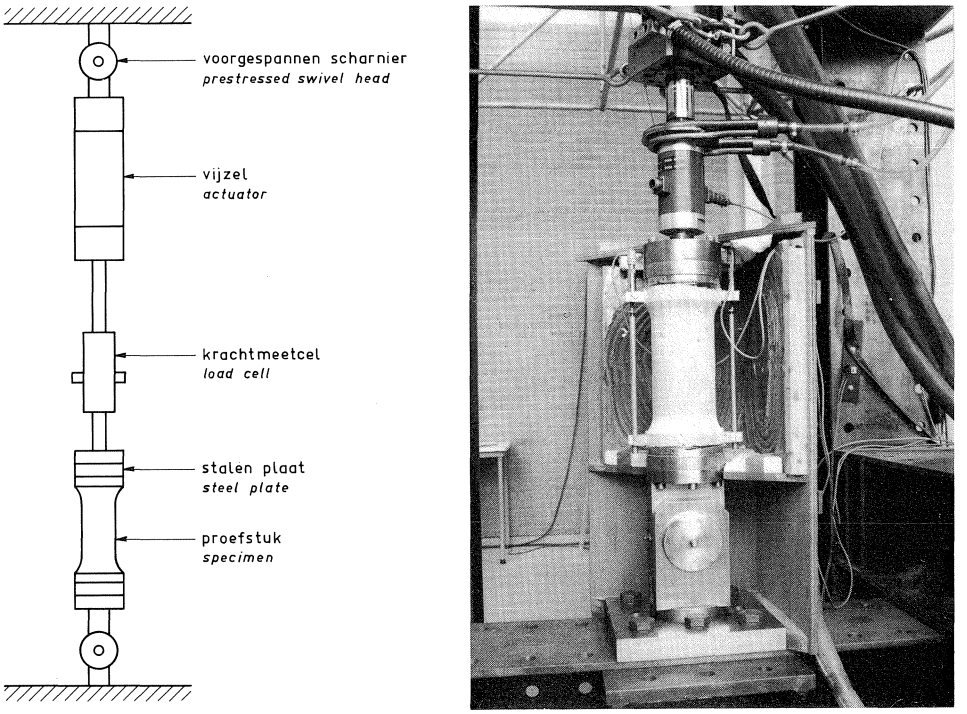

Fig. 16. Test set-up for concentric tensile testing.

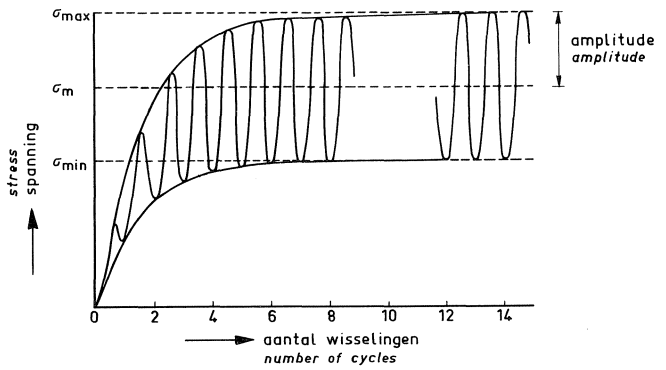

Fig. 17. The generated load signal.

During the fatigue tests the load and the associated deformation were measured eight times per cycle and stored in the memory of the computer (see Fig. 18). Next, the measured data were transferred to punched tape. This was not done for all the data, however, but always for those of two successive cycles after increasing intervals of time (see Fig. 19). The maximum interval between two measurements was established at 2^{15} cycles.

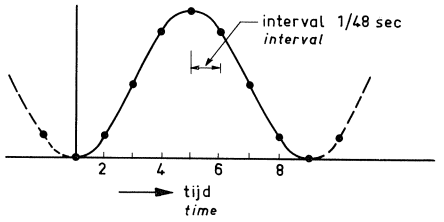

Fig. 18. The force and the associated deformation are measured eight times per cycle.

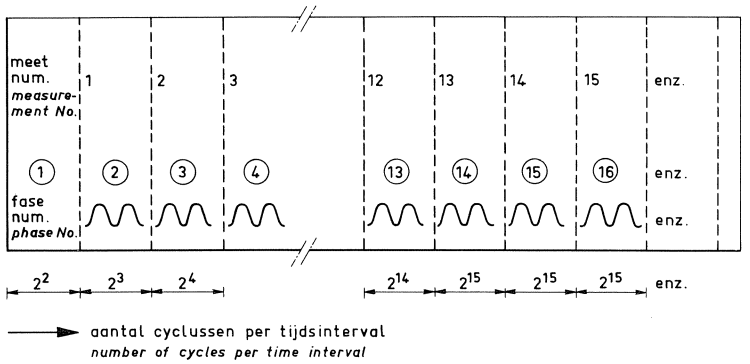

Fig. 19. Schedule of measurements.

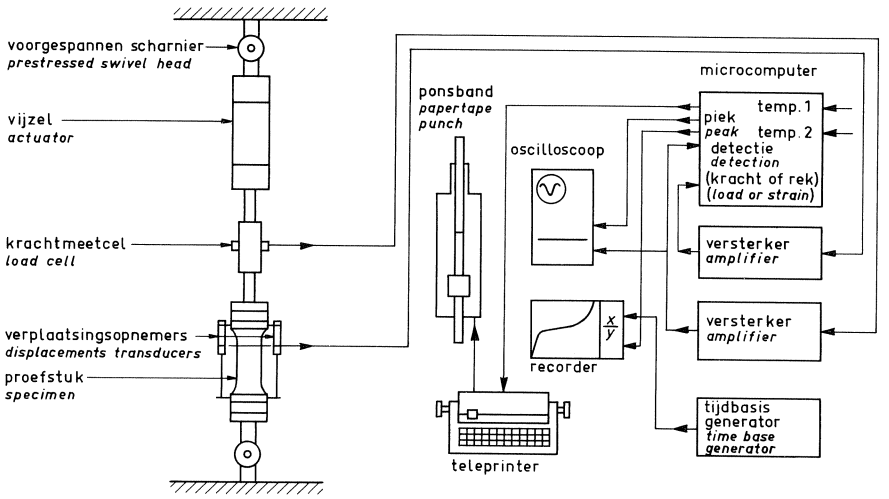

Fig. 20. Loading and control system (schematic).

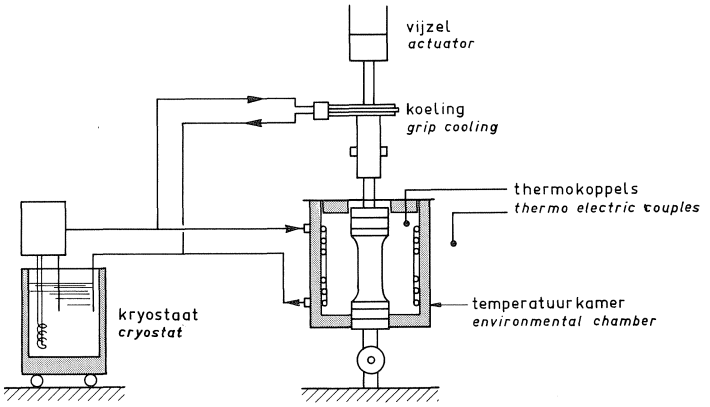

Fig. 21. Temperature control system.

However, when failure occurred, the measured data of the 50 preceding cycles were completely transferred to the tape.

Fig. 20 schematically shows the measuring system.

Since 1 °C temperature change would have caused a deformation equal to about 10% of the ultimate strain (which is 0,01%), it was necessary to enclose the specimen within a temperature-controlled chamber, in which the temperature was maintained at 21 °C $\pm$ 0,2 °C. Also, heat transmission from the jack to the specimen was prevented as much as possible (see Fig. 21).

3.2.3 Results

- S-N diagrams

The results of constant-amplitude fatigue are often represented in so-called S-N (stress-number) diagrams in which the number of cycles to failure is given as a function of parameters characterizing the dynamic loading. For the tests performed in this research the relationship is given between the number of cycles to failure and the upper limit of the relative stress (σ_{max}/f_{om}) for various values of the lower limit of the dynamic loading. The average curves, as determined for dry specimens, are represented in Fig. 22. All the individual S-N diagrams and the measured values on which they are based are given in Appendix B. As appears from Fig. 22, the fatigue life increases with a lowering of the upper limit (σ_{max}/f_{om}). The position of the lower limit (σ_{min}/f_{om} or σ_{min}/f'_{cm}) also exercises an influence. If the lower limit is so shifted that the amplitude increases, the life decreases, more particularly when the stress alternates between tension and compression. The lines indicated were determined by means of multiple linear regression analysis from the measured points. For pulsating tensile stress 177 tests and for alternating tensile-compressive stress 123 tests were analysed. For the run-outs the maximum number of cycles was adopted as the number of cycles to failure. This approach gives steeper (safer) S-N curves, as the specimens actually are able to withstand a larger

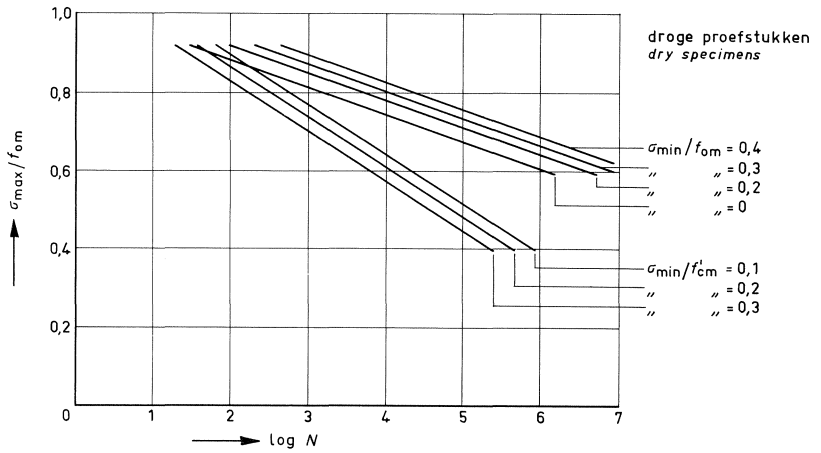

Fig. 22. Average S-N curves, for various lower limits, for dry concrete subjected to pulsating tension or to alternating tension-compression.

number of cycles. On the other hand, omitting the run-outs from the analysis would yield regression lines which would under-estimate the number of cycles to failure for these run-outs, whereas it is just this part of the S-N diagram that is most important from the practical point of view.

The following formulae were derived for the dry specimens:

- For pulsating tension ($\sigma_{min}/f_{om} \geqslant 0$):

$$\log N = 14{,}81 - 14{,}52 \frac{\sigma_{max}}{f_{om}} + 2{,}79 \frac{\sigma_{min}}{f_{om}} \tag{5}$$

The 90% confidence interval in this case was $\log N \pm 1{,}74$.

- For alternating tension-compression ($\sigma_{min}/f'_{cm} > 0$):

$$\log N = 9{,}36 - 7{,}93 \frac{\sigma_{max}}{f_{om}} - 2{,}59 \frac{\sigma_{min}}{f'_{cm}} \tag{6}$$

The 90% confidence interval in this case was $\log N \pm 1{,}38$.

From the statistical analysis it also emerged that the moisture condition of the specimen (wet or dry) had a significant effect on the life attained in pulsating tension. Partly because the dynamic load limits were referred to the static tensile strength of dry and of wet specimens respectively, the differences were small. The following formula was established for wet specimens subjected to pulsating tension:

$$\log N = 13{,}92 - 14{,}52 \frac{\sigma_{max}}{f_{om}} + 2{,}79 \frac{\sigma_{min}}{f_{om}} \tag{7}$$

This formula is valid for $\sigma_{max}/f_{om} \geqslant 0$. The 90% confidence interval was $\log N \pm 1{,}74$, just as for formula (5). For alternating tension-compression the same formula was found for

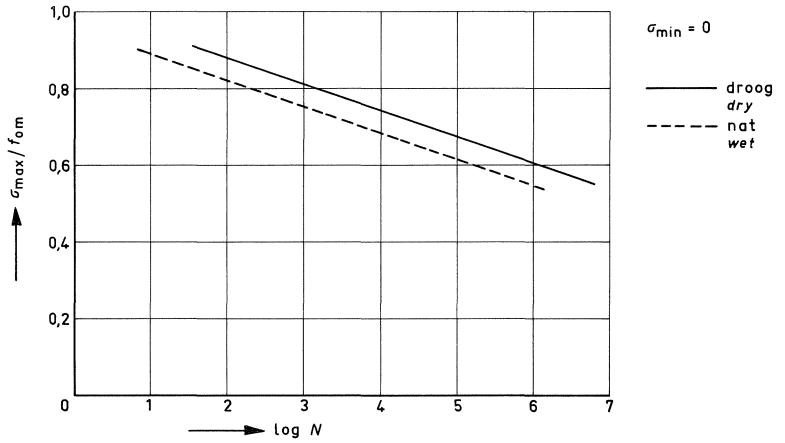

Fig. 23. S-N curves for dry and for wet concrete subjected to pulsating tension.

wet as for dry specimens, so that formula (6) must be adopted for both wet and dry.

In Fig. 23, relating to pulsating tensile tests, S-N curves for wet and for dry specimens are compared. For equal dynamic load limits a shorter life is found for wet specimens.

Note: Since the formulae (5), (6) and (7) relate to a substantial number of test results, they differ a little from similar formulae published earlier, e.g., [16], [17] and [18], because it has now been possible to determine the constants with greater accuracy.

- Scatter

Figs. 22 and 23 show average S-N curves as determined with the aid of linear regression analysis from the measured points. From the width of the confidence intervals, as indicated with reference to the formula (5), (6) and (7) and in Appendix B, it is apparent that

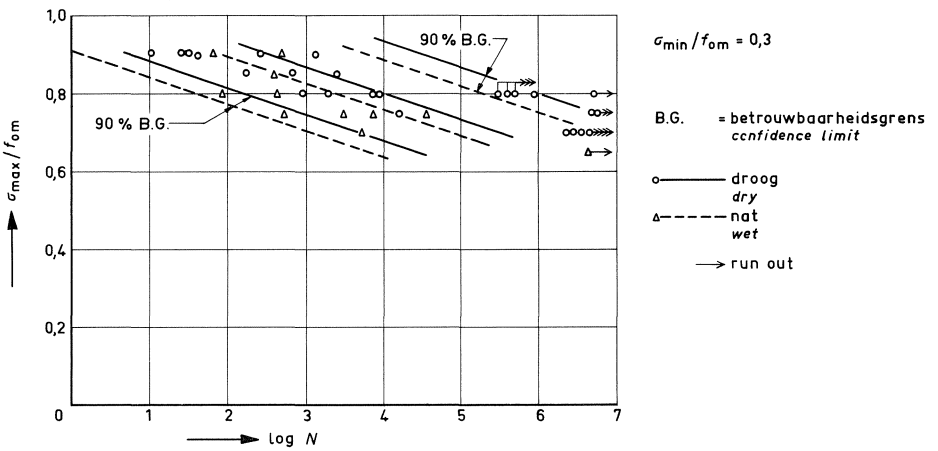

Fig. 24. Results of fatigue tests in which concrete was subjected to pulsating tension.

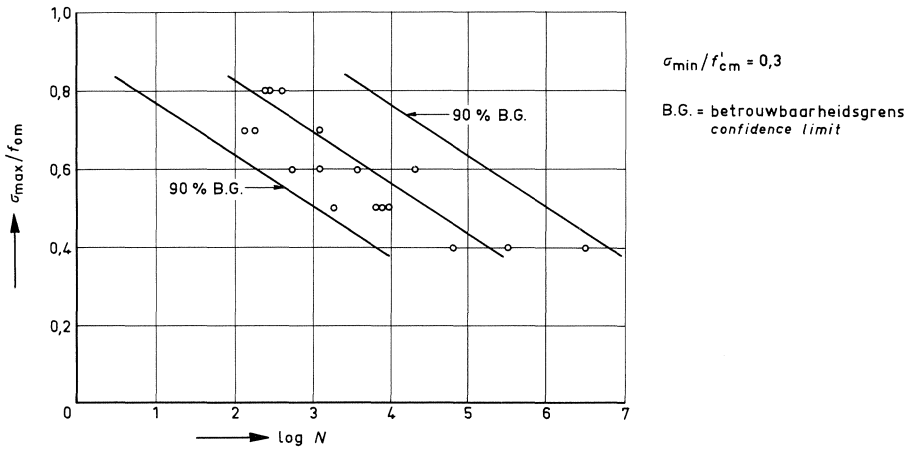

Fig. 25. Results of fatigue tests in which concrete was subjected to alternating tension and compression.

the measured results show considerable scatter (dispersion). The associated 90% confidence intervals are shown for pulsating tension in Fig. 24 and for alternating tension-compression in Fig. 25. With regard to the cause of the scatter a distinction can be drawn between, on the one hand, scatter due to the testing procedure itself and the stochastic character of fatigue and, on the other hand, scatter due to the imprecision in adjusting the stress/strength ratio at which the tests have to be performed. More particularly, the static strength of the actual specimen subjected to dynamic loading is not known, but has to be estimated from the results of static tests on other specimens made from the same batch. Since the static compressive strength and, even more so, the static tensile strength are subject to scatter, the stress/strength limits actually applied in generating the dynamic load signal will not correspond exactly to the theoretically desired limits. For example, if an upper limit (σ_{max}/f_{om}) of 80% is desired and f_{om} can vary by 10%, the upper limit actually applied will be somewhere between about 70 and 90%. Yet the result of the fatigue test is represented as relating to 80% in the S-N diagram.

It follows from the above that these effects become more pronounced when the scatter of the static strength values becomes greater. In the research it was therefore endeavoured to minimize this scatter primarily by accurate manufacture of the test specimens. Moreover, by means of a statistical method it was calculated what proportion of the scatter in the S-N diagrams is assignable to scatter of the static strength [16]. This is indicated in Figs. 26 and 27, where the shaded region within the 90% confidence interval represents the effect of scatter in the static strength. For pulsating tension the scatter is found to be caused mainly by variation of the static tensile strength. As the scatter of the compressive strength is less, in the alternating tension-compression tests the effect of the imprecision in adjusting the stress/strength ratio is less pronounced (the shaded region is therefore narrower).

The statistical analysis showed that the location of average S-N curves was not affect-

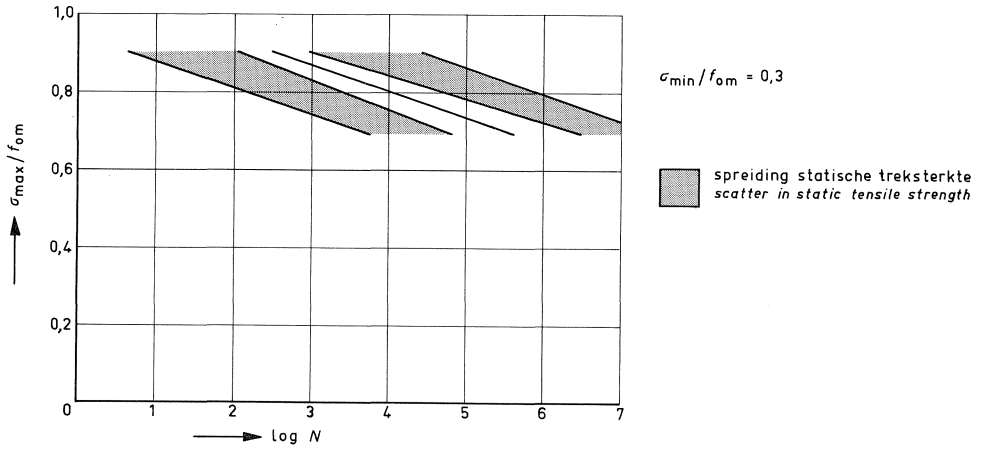

Fig. 26. Scatter of the S-N diagram for pulsating tensile stress.

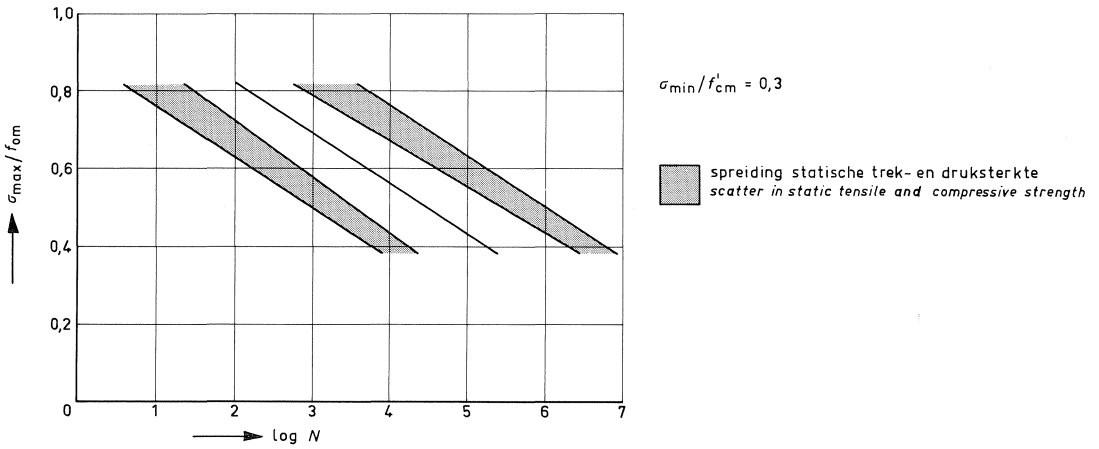

Fig. 27. Scatter of the S-N diagram for alternating tensile-compressive stress.

ed by variations in the static strength, but that only the width of the confidence region was affected [16].

For practical purposes this means that if the scatter of the static strength is taken into account by basing oneself on characteristic values, scatter in the "unsafe" direction (shorter life) is indicated chiefly by the white band under the average curve, for the probability that the actual strength will fall short of the characteristic value will then be low (e.g., 5%).

In connection with this the stress/strength ratios that actually occur will seldom be lower than assumed. However, it is of course necessary to take account of scatter due to the stochastic character of scatter, as manifested in the "white" parts of the confidence region.

- Theoretical models

It has been stated above that the longitudinal deformation was measured continuously during the constant-amplitude tests. Apart from the elastic deformation, the external deformation resulting from the loading is due partly to the growth of small internal cracks and partly to deformations such as creep occurring outside the cracking zone. At relatively high load levels the effect of crack growth is dominant, whereas creep has the greater effect at low loads. Having regard to these two aspects, the magnitude of the deformation can be linked to the degree of damage of the material. On the basis of fracture mechanics it has been deduced in [19] that, irrespective of the type of test performed, the crack length acquires a fixed value at fracture. Furthermore, adopting that starting point, a mathematical expression has been derived which is here given in a simplified form:

$$D(n) = \frac{\sigma_{max}}{f_{om}} \frac{1}{m(n)} \sqrt{1 + \varphi_{cycl}(n)} \tag{8}$$

The value of D (called the measure of destruction) ranges from the stress/strength ratio (σ_{max}/f_{om}) on application of the load (φ_{cycl} is then zero) to the value 1 at fracture. This latter statement is explained as follows. Because D is directly related to the crack length which at fracture has a fixed length and because in a static test σ_{max} is equal to f_{om}, the value of D in this case is 1, which must also apply to long-term tests (for which $\varphi_{cycl} > 0$).

In this formule $m(n)$ takes account of the change in strength of the material due to previous load cycles, so that the actual stress/strength ratio varies.

The value of $m(n)$ was determined in a separate series of tests. For this purpose the fatigue test was stopped after 100 000, 200 000 or 400 000 cycles with stress limits that allowed these respective numbers of cycles to be attained. Then the static tensile strength of the preloaded specimen was measured and was compared with the strength of non-preloaded specimens, as follows:

$$m(n) = \frac{f_0(n)}{f_{om}} \tag{9}$$

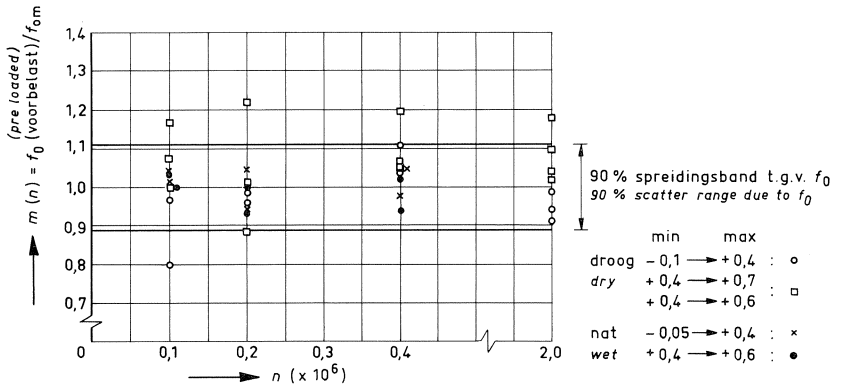

Fig. 28. Effect of preloading on the static tensile strength.

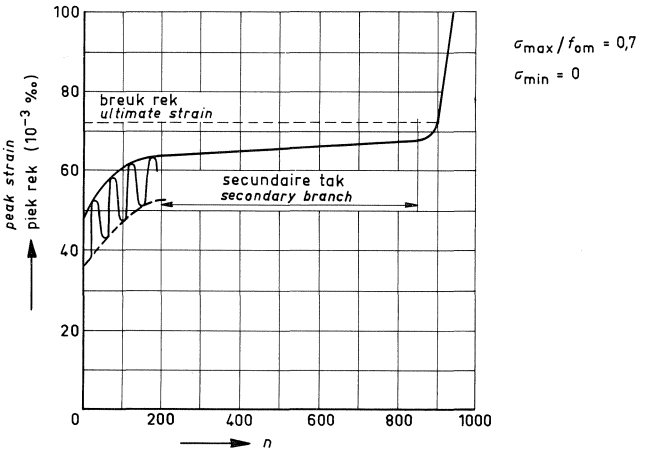

Fig. 29. Example of a cyclic creep curve.

Also, the tensile strength of the run-outs from the preceding fatigue tests, in which the number of cycles was generally about 2×10^6, was compared with the static strength of the non-preloaded specimens.

The results are summarized in Fig. 28, from which it appears that the average value of $m(n)$ was equal to 1 and that the scatter could be explained in terms of the scatter of the tensile strength. Therefore the value $m(n) = 1$ can be adopted for the fatigue tests performed in this research.

Accordingly, the following formula was used for calculating $D(n)$ at failure:

$$D(n=N) = \frac{\sigma_{\max}}{f_{\text{om}}} \sqrt{1 + \varphi_{\text{cycl}}(n=N)} \tag{10}$$

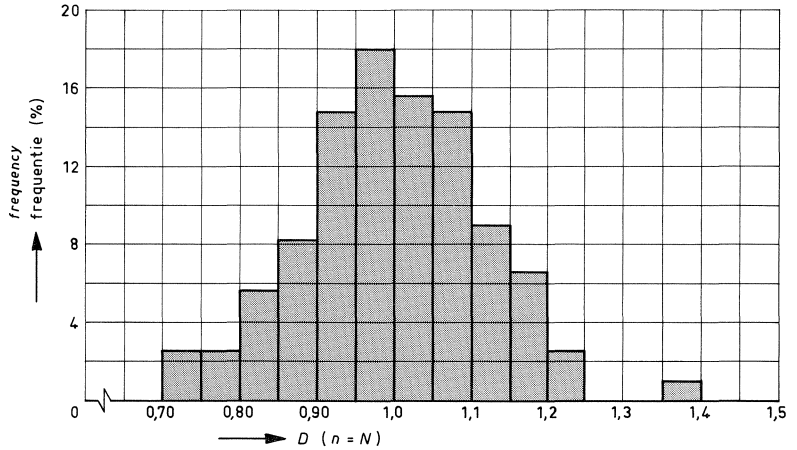

Fig. 30. Distribution of D from formula (10) at failure.

The cyclic creep coefficient was calculated from the total peak strain (ε_{tot}) at failure in the tensile range of the cycle (see Fig. 29) and from the elastic strain (ε_e) at σ_{max} by making use of the modulus of elasticity as determined in the static tensile tests:

$$\varphi_{cycl}(n=N) = \frac{\varepsilon_{tot}(n=N) - \varepsilon_e}{\varepsilon_e} = \frac{\varepsilon_{tot}(n=N) - (\sigma_{max}/E_{bm})}{(\sigma_{max}/E_{bm})} \tag{11}$$

In this way $D(n)$ at failure was calculated for 122 fatigue tests. The result is presented in the histogram in Fig. 30. The average value was 0,99 and the coefficient of variation was 10,0%.

It can be inferred that with D as the criterion of failure the magnitude of φ_{cycl} is a measure of the internal damage of the specimen.

From formula (10) it can furthermore be deduced that, for equal σ_{max}/f_{om}, wet concrete - which undergoes more creep - will attain a shorter fatigue life than dry concrete. This was confirmed experimentally (see Fig. 23).

Also, with decreasing frequency of cyclic loading, the creep per cycle will become greater, so that then, too, shorter fatigue life must be expected. This was verified in a series of tests in which the frequency applied was 0,06 Hz. In the S-N diagram given in Fig. 31 the average results obtained at 6 Hz are compared with those obtained at 0,06 Hz. In the latter case the values found for the life were lower. (The results of the tests at 0,06 Hz are presented in Appendix C).

Starting from a fixed crack length at failure, there must be a relation between the increase in crack length per cycle and the number of cycles to failure. This crack length increase can be determined from the slope of the secondary branch of the cyclic creep curve where the strain on attainment of the maximum tensile stress in each cycle has been plotted as a fuction of the number of cycles (see Fig. 29). In the case of alternating tension-compression the strain corresponding to the change in the algebraic sign of the stress in the ascending branch was adopted as zero. As with other materials, there is

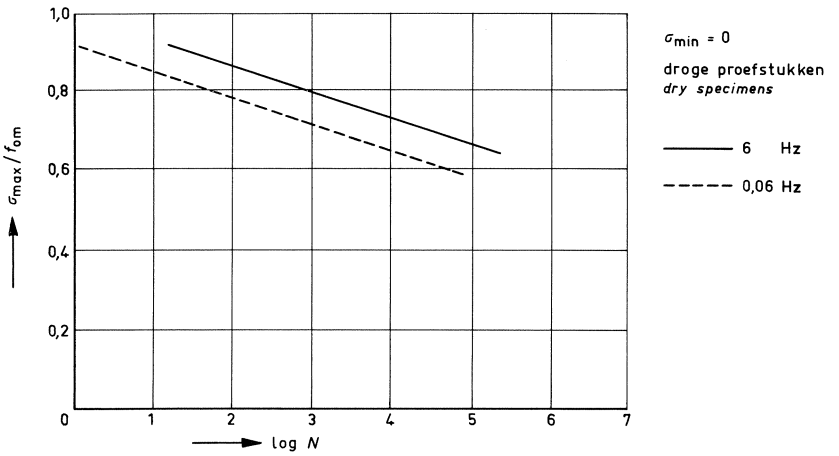

Fig. 31. Influence of testing frequency on the number of cycles to failure.

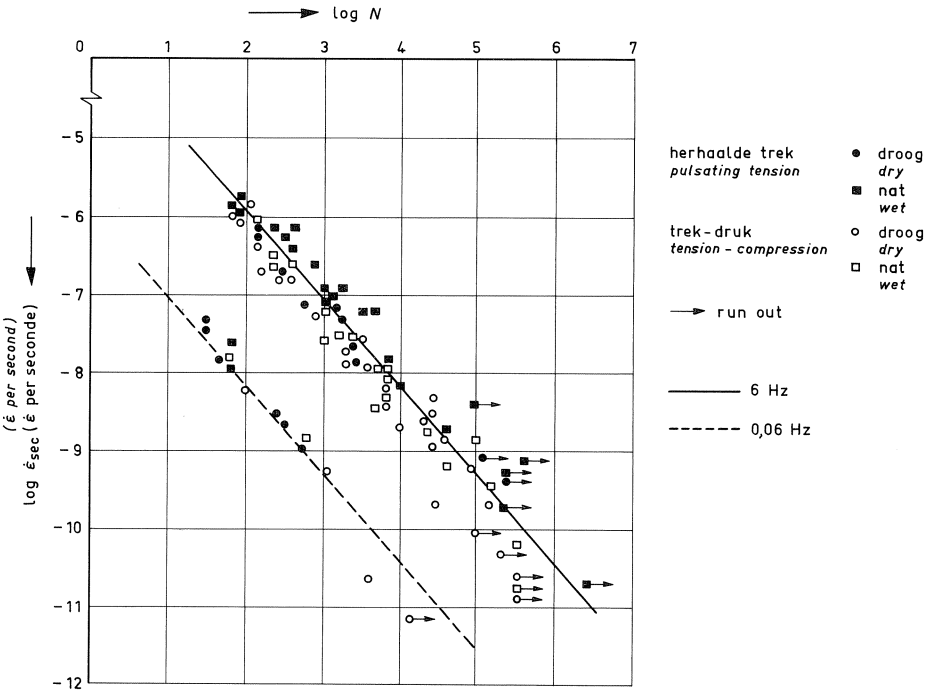

Fig. 32. Relation between the secondary creep rate ($\dot{\varepsilon}_{sec}$) and the number of cycles to failure (N).

found to exist a linear relation between log $\dot{\varepsilon}_{sec}$ and log N (the fatigue life).

This relation is shown for 6 Hz and for 0,06 Hz in Fig. 32. With diminishing secondary creep rate ($\dot{\varepsilon}_{sec}$) the fatigue life increases, as can be described by the following formula for the constant-amplitude tests at 6 Hz:

$$\log N = -3{,}25 - 0{,}89 \log \dot{\varepsilon}_{sec} \tag{12}$$

This formula is applicable to dry as well as to wet specimens and is valid both for pulsating tension and for alternating tension-compression. As emerges from the Figure, the scatter is small. So a prediction of the number of cycles to failure based on $\dot{\varepsilon}_{sec}$ is more accurate than based on stresses in an S-N diagram. An explanation is the fact that $\dot{\varepsilon}_{sec}$ is a representation of the actual damage in the material.

Fig. 32 shows that for equal secondary creep (per unit time) the number of cycles to failure at 0,06Hz is approximately 100 times less at 6 Hz. The length of time up to failure is therefore about the same in both cases.

So, for equal $\dot{\varepsilon}_{sec}$, the failure time is found to be independent of the frequency - whether this is 6 Hz or 0,06 Hz. However, for given values of relative σ_{min} and σ_{max}, the frequency does affect the magnitude of $\dot{\varepsilon}_{sec}$, which is smaller for lower frequency. This is apparent, inter alia, from Fig. 31, where lowering the frequency by a factor of 100 causes the number of cycles to failure to be reduced by a factor of 30, not 100 (log 30 = 1,5).

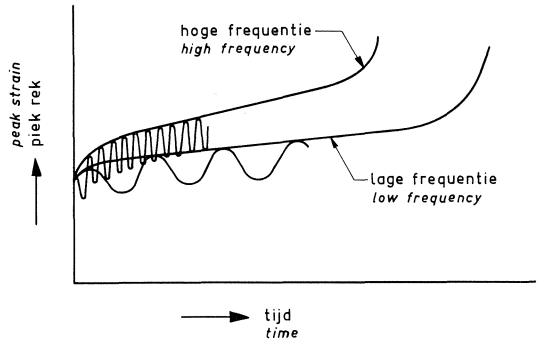

Fig. 33. Cyclic creep curves for 6 Hz and 0,06 Hz.

These features are further clarified in Fig. 33, where the peak strain values have been plotted against time. At the low frequency the time up to failure is longer (longer life) because $\dot{\varepsilon}_{sec}$ has decreased in relation to its value at the high frequency.

If no direct measure for $\dot{\varepsilon}_{sec}$ is available, this quantity will have to be determined from a relationship with the stresses, the frequency and other influencing factors.

3.3 *Flexural tension*

3.3.1 General

Bending tests were performed in which the bottom fibre stress varied between two predetermined limits. The upper limit was chosen between 40% and 90% of the static flexural (tensile) strength (modulus of rupture), while the lower limit was 0, 10, 20 or 30% of the static compressive strength. The fatigue tests were characterized by sinusoidal constant-amplitude load cycles applied at a frequency of about 8 Hz. The number of cycles was limited to a maximum of 2×10^6.

The tests were performed on specimens which, after manufacture, were stored in a humidity chamber at 20 °C and not less than 90% relative humidity for 1 week and in an air-conditioned room at 20 ± 1 °C and 60 ± 2% relative humidity for a further 3 weeks.

3.3.2 Test procedure

The limit σ_{min} and σ_{max} between which the bottom fibre stress varied were referred to the static compressive strength and the flexural strength of the concrete. In principle, these strengths were determined from the average results of compressive and flexural tests on specimens made from the same batch of concrete as that from which the corresponding fatigue test specimens were made. The compressive strength was determined on three 200 mm cubes and the flexural strength on three 150 mm × 150 mm × 600 mm prisms by means of a three-point bending test.

Earlier research [20] had shown, however, that a possible explanation for the con-

siderable scatter of fatigue test results might be found in the scatter of the flexural strength values of concrete ($V(f_c) \cong 12{,}1\%$).

Therefore Committee C 33 decided to determine the upper stress limit σ_{max} on the basis of the actual flexural strength of each dynamically tested specimen. For this purpose dimensions of 150 mm × 280 mm × 2300 mm were adopted for these specimens. By applying the load at the one-third span point (see Fig. 39) it was possible first to determine the flexural strength of the concrete in a static test without causing the stress at the section subsequently investigated for fatigue (dynamic test) to exceed half the flexural tensile stress. The flexural strength was determined from the difference between the cracking moment of the prestressed specimen, as determined in an initial static bending test (i.e., on the uncracked specimen), and the destressing moment (i.e., the bending moment at which the crack re-opens) in a second test.

In order to achieve the desired upper and lower limits of the stress (in the bottom fibre), the specimens were prestressed at the bottom edge of the core (or kern) of the section by means one, two of three non-bonded strand tendons (type U.T.-12.7 Z). The position of these tendons is shown in Fig. 35. The specimens were prestressed when they were 7 days old, in order to reduce the effect of concrete creep and prestressing steel relaxation during the fatigue test.

The concrete mix composition used for making the test specimens is indicated in Table 4.

Table 4. Concrete mix composition for the flexural tensile tests

type of cement	portland cement class B
cement content	350 kg/m^3
aggregate (gravel + sand)	1930 kg/m^3
water-cement ratio	0,46
maximum particle diameter	14 mm

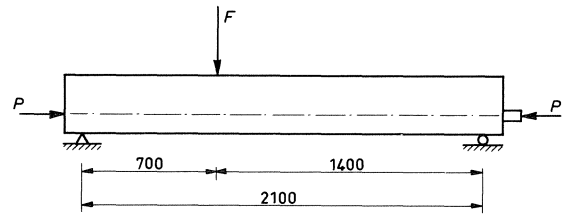

Fig. 34a. Loading arrangement for static bending test.

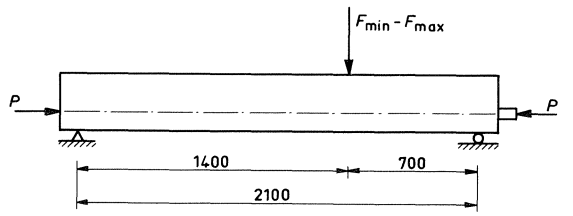

Fig. 34b. Loading arrangement for dynamic bending test.

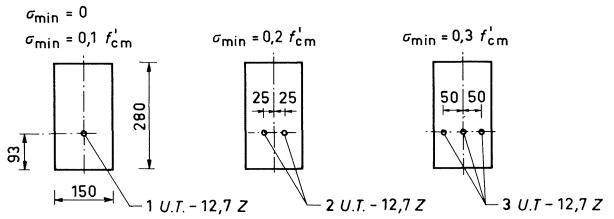

Fig. 35. Location of the prestressing tendons.

The prestressed specimen was mounted on two hinge-type bearings, one of which was fixed and the other was free to move horizontally (see Fig. 34).

Loading was applied with the aid of a hydraulic jack connected to a pulsator (frequency approx. 8 Hz) with sinusoidal load variation between two predetermined limits (F_{min} and F_{max}). The prestressing force P and the forces F were accurately measured by means of load cells. The load limits and the magnitude of the prestress were so chosen that the bottom fibre stress under the combined influence of dead weight (p), prestressing force (P) and applied forces (F_{min}, F_{max}) varied between the desired limits σ_{min} and σ_{max} without the compressive stress in the top fibre (under the action of F_{max}) exceeding 40% of the comprssive strength (see Fig. 36). This relatively low value of the compressive stress can be presumed not to give rise to fatigue failure. The stresses were in all cases calculated in accordance with linear elastic theory.

The cracking load in the static tests and the instant of cracking in the fatigue tests were determined with a series of four electrical resistance strain gaugus (type KYOWA KC 70, 68 mm gauge length) connected in a bridge circuit. These gauges were affixed to the underside of each specimen at the two cross-sections which were most severely stressed either in the static or in the fatigue test. The experimental set-up with which

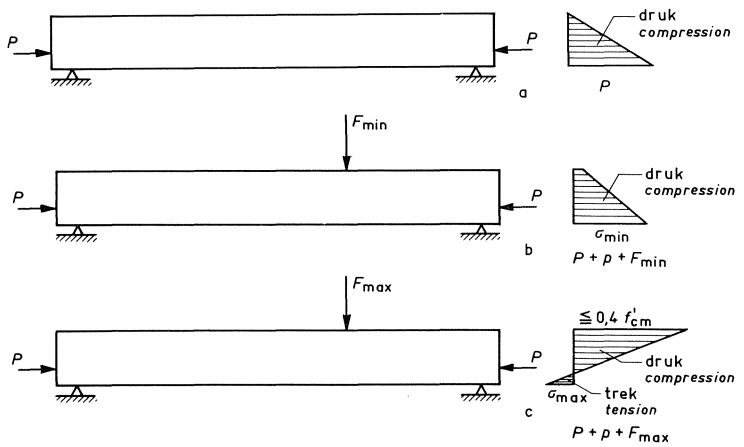

Fig. 36. Stress distributions associated with the various loads.

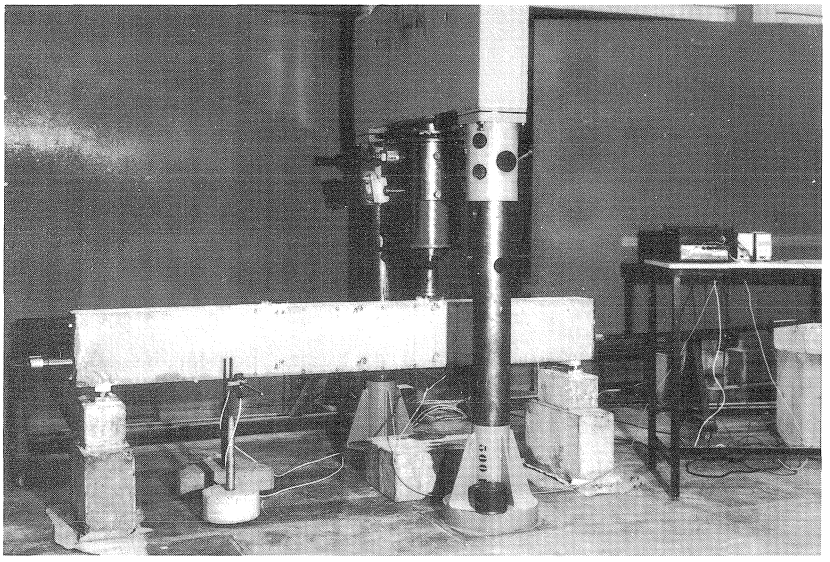

Fig. 37. Experimental set-up for the flexural tests.

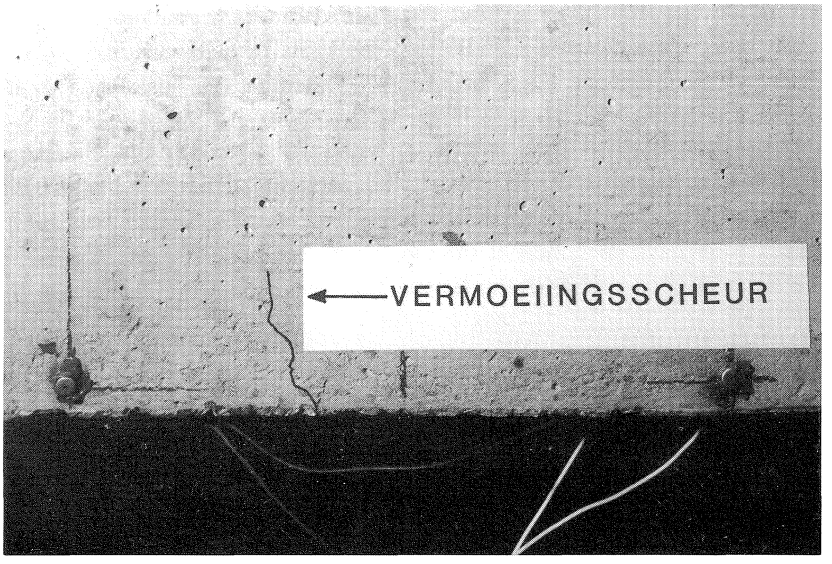

Fig. 38. Fatigue crack.

he beams were tested statically and dynamically is shown in Fig. 37. A detail view of a specimen cracked under fatigue loading is given in Fig. 38.

For further information on the materials employed (concrete and steel) and on the strain measurements performed on the concrete in connection with the prestress the reader is referred to [12]. A more detailed description of the electronic equipment for the detection of fatigue cracks is given in Appendix D.

3.3.3 Results of static tests

The results of the static tests performed on the hardened concrete (at 28 days) are summarized in Table 5.

Table 5. Average values from the static tests (RUG)

dimensions of specimens (mm)	compressive strength f'_{cm} 200 × 200 × 200	flexural strength f_{cm} 150 × 150 × 600	modulus of elasticity E'_{bm} 200 × 200 × 500
average (N/mm²)	49,2	4,40	36300
coefficient of variation (%)	4,3	8,3	3,3

Averaged over a total of 74 batches of concrete the cube strength is 49,2 N/mm² ($V(f'_c) = 4{,}3\%$) and the flexural strength 4,40 N/mm² ($V(f_c) = 8{,}3\%$). The loading rate was 1 N/mm² · s in the compressive (cube) tests and 0,2 N/mm² · s in the flexural tests.

The static modulus of elasticity at 25% of the compressive strength, determined on 200 mm × 200 mm × 500 mm prisms, is also indicated in the table. The results of the flexural fatigue tests on the specimens are summarized in Appendix E, which moreover contains an overview of the characteristics of the hardened concrete.

Note: In connection with the investigations under concentric tension the compressive strength was determined on 150 mm cubes, whereas 200 mm cubes were used for the purpose in connection with the flexural tension investigations. The conversion factor for the cube strengths is:

$$\frac{f'_{cm,150}}{f'_{cm,200}} = 1{,}05 \tag{13}$$

The effect of this difference in cube size on the location of the S-N curves is practically negligible.

3.3.4 Results of fatigue tests

- S-N diagrams

The results of the 120 constant-amplitude tests are represented in S-N diagrams. For the various values of σ_{min} the ratio σ_{max}/f_c has been plotted against log N and the regression lines (S-N curves) for the measured points have been determined (see Fig. 39 and Table 6). The individual S-N diagrams and the measured points on which they are based are given in Appendix F. For the run-outs the maximum number of cycles was, in the analysis, taken as equal to the number of cycles to cracking (in analogy with the approach adopted in the concentric tension investigations). The reasons for proceeding in this way are stated in Section 3.2.3 of this report.

In order to establish a general equation for the S-N curves the tension-compression

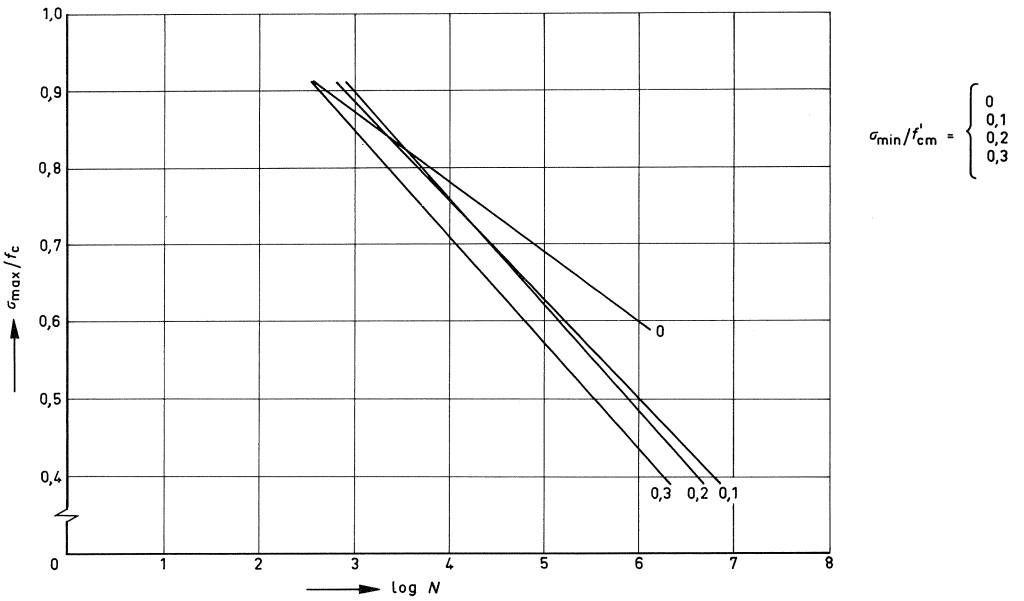

Fig. 39. S-N curves for various levels of σ_{min}/f'_{cm}.

Table 6. Regression equations of the S-N curves for flexural tension

lower limit σ_{min}/f'_{cm}	regression equation	correlation coefficient
0,0	$\log N = 12{,}53 - 10{,}95 \frac{\sigma_{max}}{f_c}$	− 0,86
0,1	$\log N = 9{,}92 - 7{,}82 \frac{\sigma_{max}}{f_c}$	− 0,89
0,2	$\log N = 9{,}52 - 7{,}29 \frac{\sigma_{max}}{f_c}$	− 0,87
0,3	$\log N = 9{,}19 - 7{,}32 \frac{\sigma_{max}}{f_c}$	− 0,92

test results, on the one hand, and the pulsating tension test results, on the other, were analysed separately. In this way the following formulae were derived:

- For pulsating tension with zero lower limit ($\sigma_{min}/f'_{cm} = 0$):

$$\log N = 12{,}53 - 10{,}95 \frac{\sigma_{max}}{f_c} \tag{14}$$

The correlation coefficient in this case is − 0,86 for 31 observations, and the confidence interval is: $\log N \pm 1{,}19$.

- For alternating tension-compression $(\sigma_{min}/f'_{cm} > 0)$:

$$\log N = 9{,}91 - 1{,}93 \frac{\sigma_{min}}{f'_{cm}} - 7{,}45 \frac{\sigma_{max}}{f_c} \tag{15}$$

The multiple correlation coefficient is $-0{,}89$ for 89 observations, and the confidence interval is: $\log N \pm 1{,}03$.

The four S-N curves calculated with the formulae (14) and (15) are represented in Fig. 40.

As appears from this diagram, the number of cycles to failure increases with decreasing upper limit of the variable stress (σ_{max}/f_c). When the S-N curves shift to higher values of the lower limit (σ_{min}/f'_{cm}), the fatigue life decreases. This means that the alternation between tension and compression has a more damaging effect on the concrete according as the compressive stress in the bottom fibre is greater.

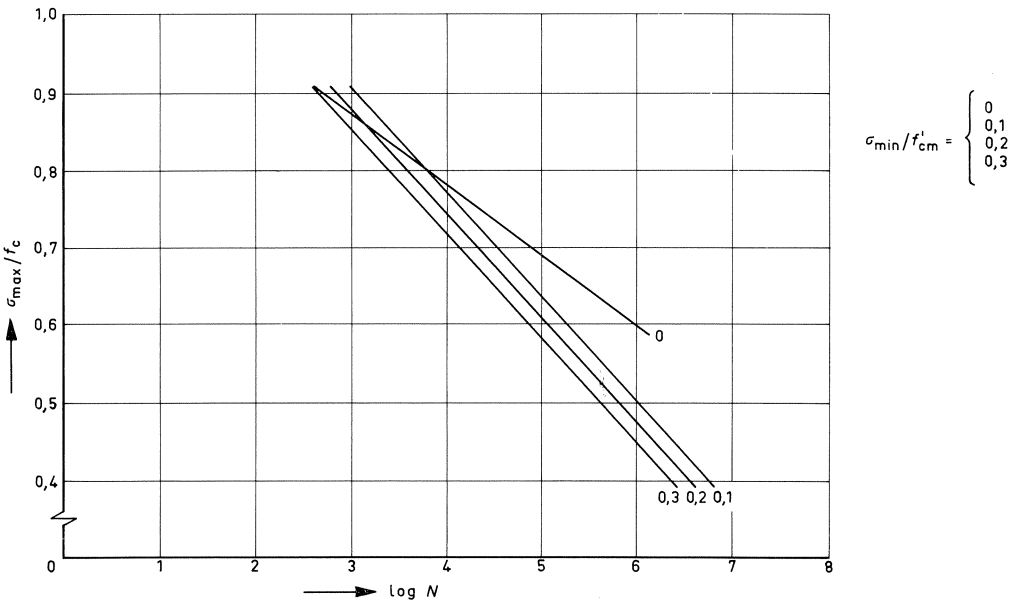

Fig. 40. S-N curves for alternating flexural tensile-compressive loading, calculated with formulae (15) and (16).

- Scatter

In Fig. 41, which shows the S-N diagram for $\sigma_{min} = 0{,}3 f'_{cm}$, the average line determined by means of linear regression analysis from the measured points is indicated. It is apparent that the test results are subject to considerable scatter. For a more detailed discussion of the scatter occurring in fatigue tests the reader is referred to Section 3.2.3 relating to concentric tension.

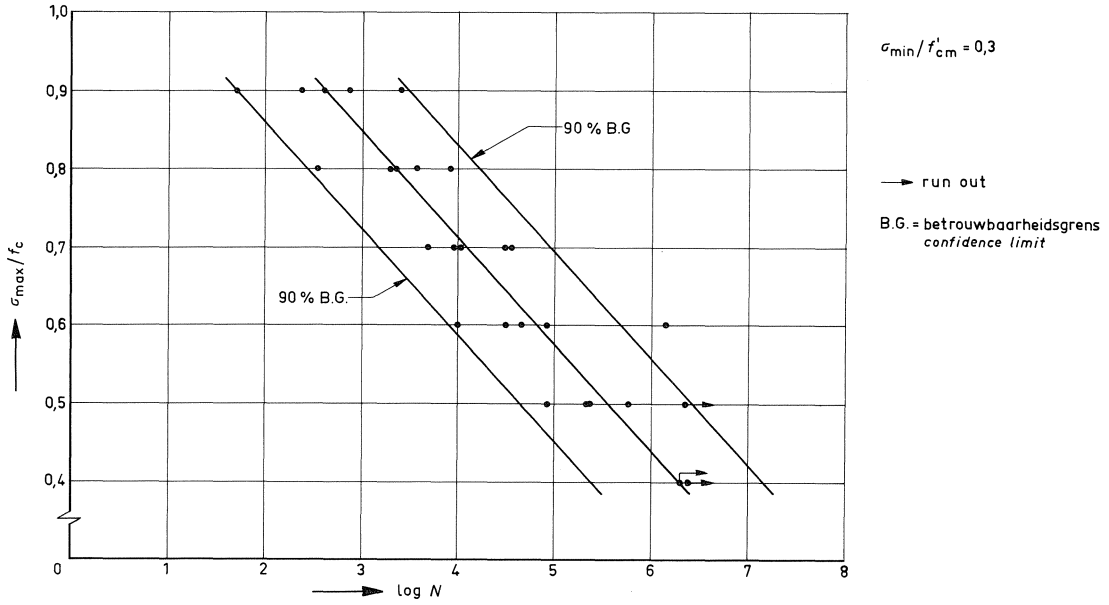

Fig. 41. S-N curve for $\sigma_{min}/f'_{cm} = 0{,}3$.

4 Discussion of the results of the constant-amplitude tests

4.1 *Concentric tension as compared with flexural tension*

Fig. 42 shows two S-N diagrams established for the purpose of comparison of the results obtained from the concentric tension and the flexural tension tests respectively. In Fig. 42a the lower limit of the variable (pulsating) stress is zero, whereas in Fig. 42b the lower limit of the variable (alternating) stress is equal to 30% of the compressive strength. In both cases, on the basis of equal stress/strength ratio at the start of testing, the fatigue life attained in the flexural test is longer than in the concentric test. This conclusion is justified despite the scatter found to occur.

Because in the two types of test the stress at the start of testing was referred to the concentric (direct) tensile strength and the flexural strength (modulus of rupture) respectively, the differences must be attributed to the changes that occurred during the execution of the fatigue tests themselves.

In a three-point bending test the stress in the bottom fibre of the specimen will have its maximum value directly under the point of application of the load and will decrease towards the supports. The concrete will not have the same value at every point along the bottom of the specimen. Therefore the first crack may occur a some distance from the section of maximum bending moment (see Fig. 43). As a result, the stress in the zone adjacent to the crack will decrease, and cracking in these zones will occur later. By detecting the crack precisely at the section where the flexural stress has its maximum

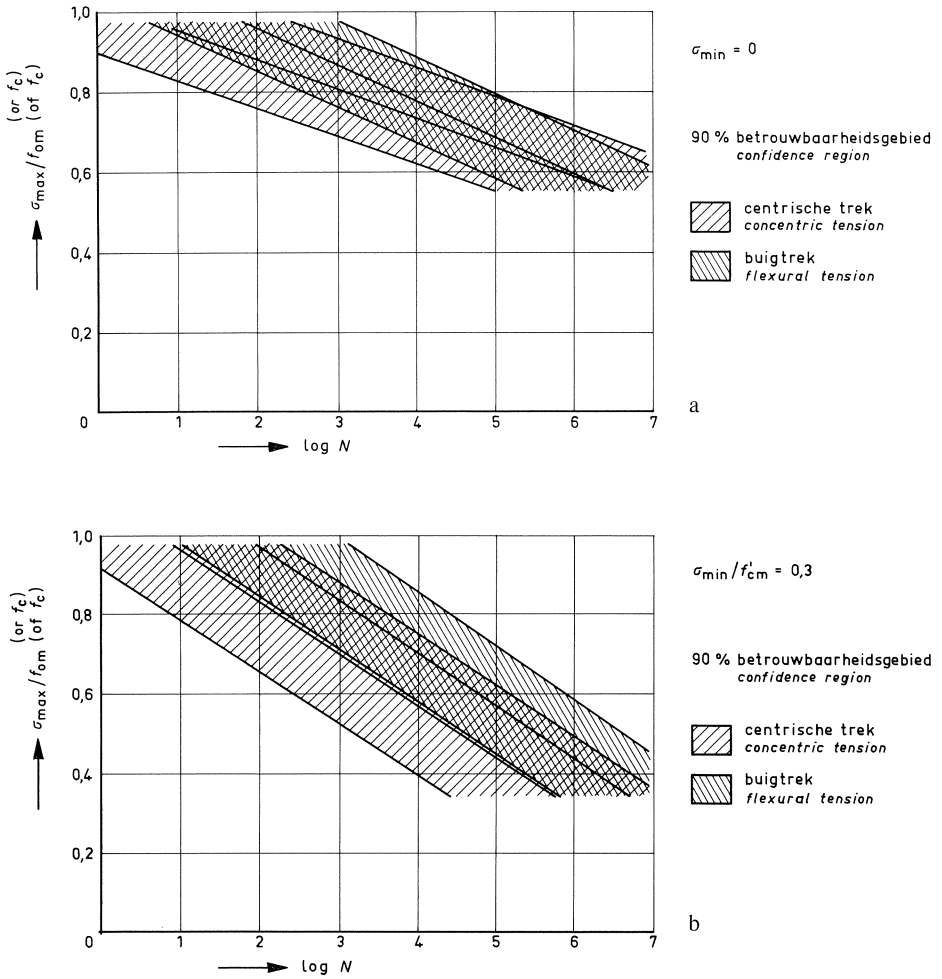

Fig. 42. Comparison between S-N curves for concentric tension and flexural tension.

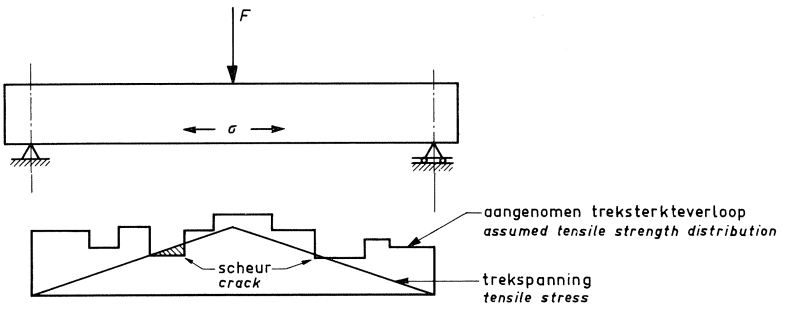

Fig. 43. Possible location of first cracks.

value and taking this as the criterion for estimating the fatigue life we obtain a more favourable conception of the behaviour in comparison with concentric tensile fatigue testing in which the stress is constant over the cross-section and a crack immediately leads to failure.

In addition to the effect of the scatter of the tensile strength along the bottom of the specimen loaded in bending, the stress gradient at the cross-section is found also to affect the life.

Experiments in which concrete was loaded concentrically and eccentrically in compression revealed that in proportion as the eccentricity and therefore the stress gradient increased, more cycles to failure were attainable [22]. This is apparent from Fig. 44, where the result of concentric tests ($e = 0$) and eccentric tests ($e = \frac{1}{18}$ and $\frac{1}{6}$ times the width of the test prism) are represented.

Since there is a stress gradient in the flexurally loaded as distinct from the concentrically loaded specimens, the former can, in view of what is stated above, be expected to attain longer fatigue lives.

The effect of the stress gradient on the fatigue of concrete was the subject of further investigation, as reported in [23]. It appears that the stress gradient existing at the commencement of the test produces a strain gradient. During a fatigue test, as also in a creep test, the stress relaxation that occurs will be greatest in the fibres which undergo the greatest amount of strain. This relaxation causes a redistribution of the stress, a process in which the fibres located further inwards from the extreme fibre increasingly participate in carrying the load. This effect, which applies to compression as well as to tension, is more pronounced according as the stress gradient increases or, in the case of flexural load, according as the depth of the beam is less.

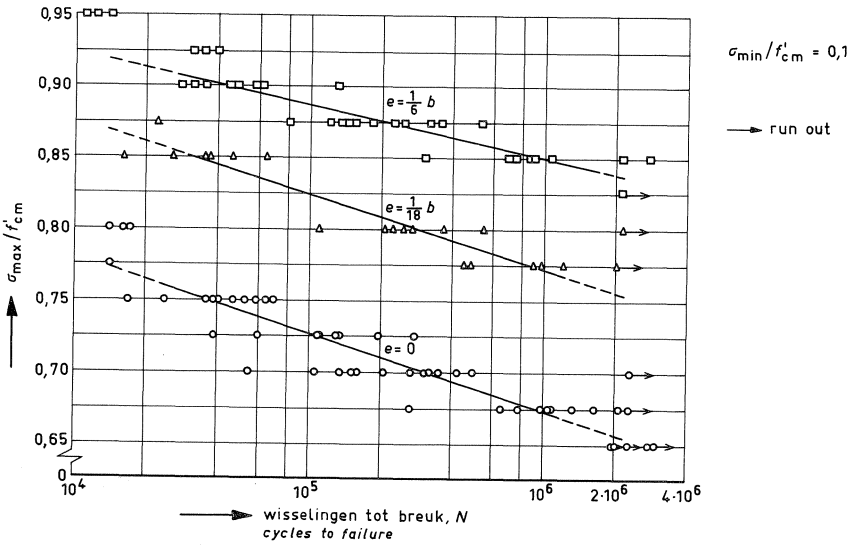

Fig. 44. Effect of the eccentricity e on the number of cycles to failure, according to OPLE en HULSBOS [22].

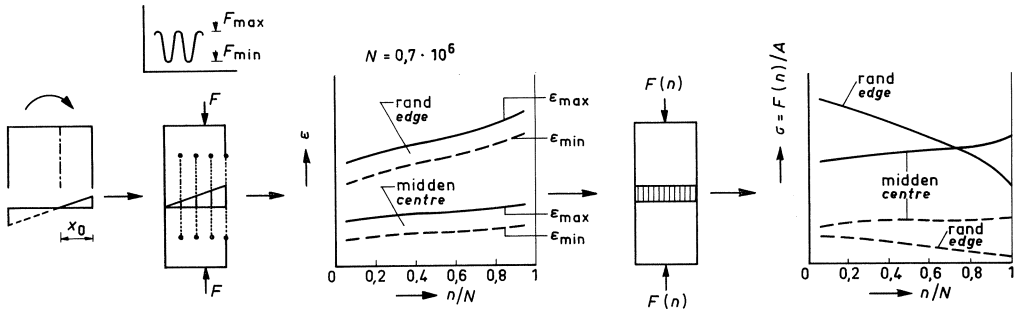

Fig. 45. Determination of the stress distribution in eccentrically loaded sections, according to DILLMANN [23].

The associated stresses were determined by carrying out eccentric dynamic compressive tests in which the deformations at various fibres were measured and then carrying out concentric compressive tests in which the deformation "history" measured per fibre was used to control the testing operation (see Fig. 45). The result is presented in Fig. 46, which shows that with increasing number of cycles (n/N increasing) the stress at the outermost fibre decreases and the stress maximum shifts towards the neutral axis ($x = 0$).

From what precedes it can be inferred that, starting from a particular stress distribution at the beginning of the test, a shorter fatigue life must be expected if stress redistribution can take place. This is so if a stress gradient exists, as in a flexural test.

This explains, qualitatively anyway, the difference in fatigue life attained in the case of concentric tension and of flexural tension respectively. A quantitative study of this effect will require a closer insight into the redistribution of the stresses, which will have to be obtained from systematic experimental research.

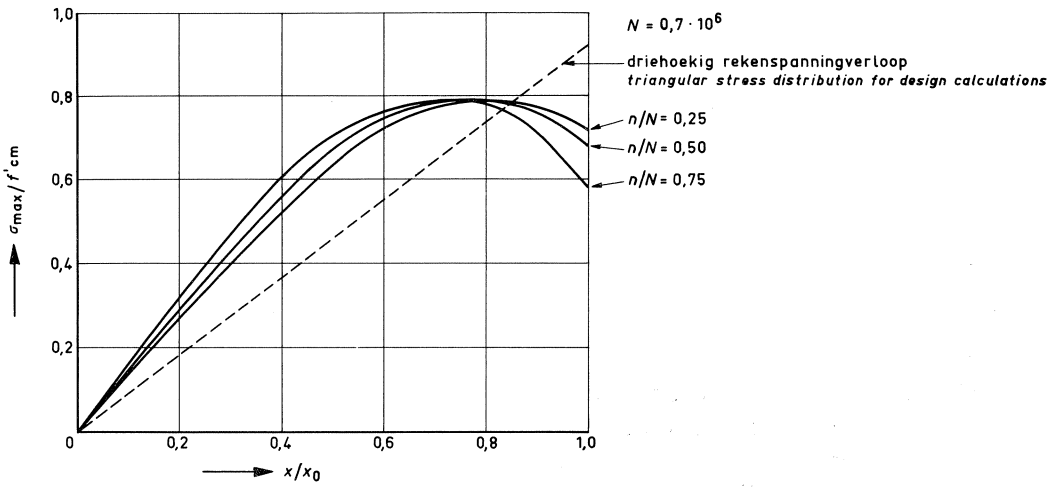

Fig. 46. Stress distribution in the flexural tensile zone, according to DILLMANN [23]. (x_0 = distance from neutral axis to extreme fibre).

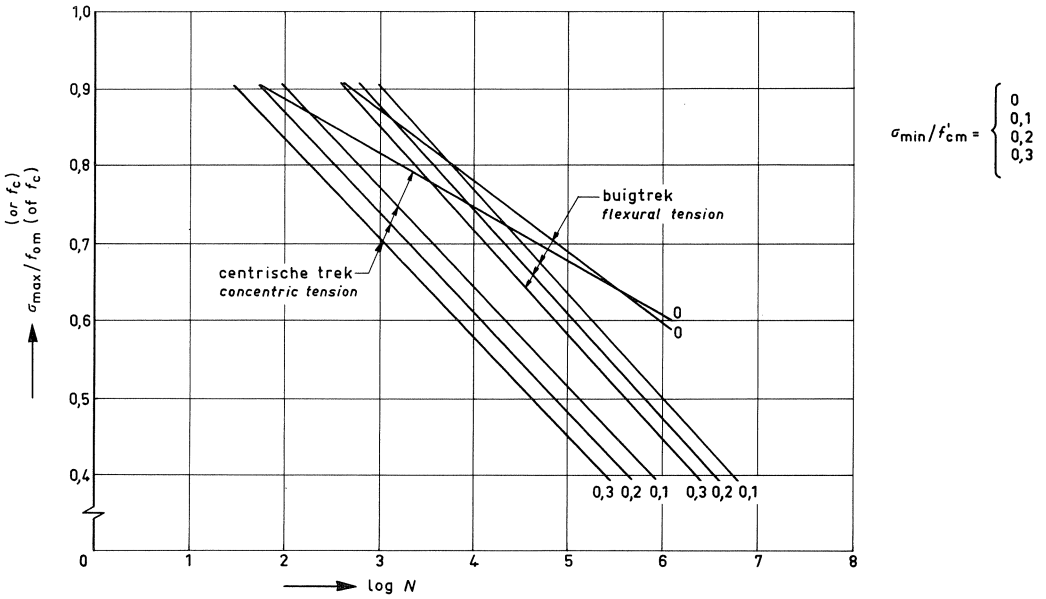

Fig. 47. Comparison of the S-N curves as determined for concentric tension (THD) and flexural tension (RUG).

Finally, the procedures adopted in determining the S-N curves from the measured data call for some comment. In both the concentric tension and in the flexural tension tests a distinction was drawn between tests performed in the tensile range only (pulsating stress) and those performed in the tensile and compressive ranges (alternating stress). The tests with pulsating stress with zero lower limit were conceived as repetitive tensile tests. In the flexural testing program the tests were predominantly of the alternating (tension-compression) type, and for this reason the results of the tests with zero lower limit were also analysed separately.

The results of the two analyses, for the lower limit $0{,}0f'_{cm}$, $0{,}1f'_{cm}$, $0{,}2f'_{cm}$ and $0{,}3f'_{cm}$, are summarized in Fig. 47. It appears from this diagram that in both cases the effect of the lower limit is clearly manifest.

4.2 *Comparison with the literature*

4.2.1 Concentric tension

As already stated in the review of the literature, the results of two research projects in which concrete or mortar was subjected to uniaxial repetitive loading in tension have been reported in earlier publications [4, 5]. However, because of differences in the conditions of testing, they are only tentatively comparable with the THD research results.

The S-N curves published in the literature and an S-N curve obtained from the THD tests are given in Fig. 48. Having regard to the scatter inherent in such test results, there

is good agreement. This leads to the conclusion that more particularly the stress/strength ratio influences the fatigue behaviour.

Earlier publications reporting uniaxial concentric tension-compression tests are not known. However, basing himself on splitting tensile tests, Tepfers [15] came to the conclusion that the alternation of stress from tension to compression, and vice versa, does not result in additional damage. This is not in agreement with the results yielded by the THD tests. The S-N curve deduced by Tepfers is given in Fig. 49, the lower limit of the stress being zero in this case. The results of the tension-compression (alternating stress) tests performed in the THD research are also included in that diagram, from which it appears that the fatigue life is over-estimated if it is based on the curve for $\sigma_{min} = 0$ in the case of tension-compression.

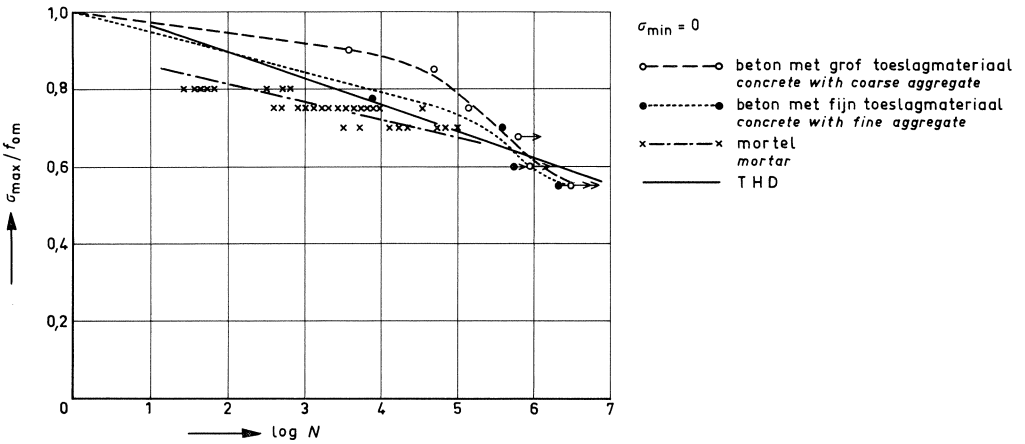

Fig. 48. Comparison of the results of fatigue tests with concentric tension (THD) with data published in the literature.

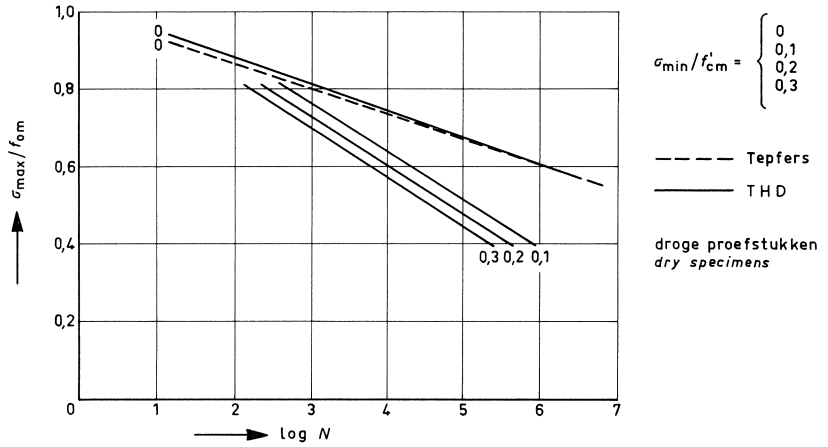

Fig. 49. S-N curve for $\sigma_{min} = 0$ over-estimates the life in fatigue tests in which the stress alternates between tension and compression.

4.2.2 Flexural tension

It has been noted in the review of the literature that only a small number of data relating to flexural tension-compression tests have been published. A distinction should be drawn between flexural tests in which the bottom fibre stress varies between zero and a tensile stress (pulsating stress) [6, 7] and those in which the stress alternates between a tensile stress and a compressive stress of equal absolute magnitude [9, 10, 11, 12].

Raithby [6] reports the results of flexural tests - four-point bending tests on beams - in which the lower limit of the stress was zero and the upper limit was referred to the static flexural strength (modulus of rupture). Three different concrete mixes were tested, at different ages. The test results are represented in the form of an average S-N curve in Fig. 50, where the corresponding curve for $\sigma_{min} = 0$ based on the RUG research is also given.

It appears from this diagram that the S-N curve obtained by RUG is in good agreement with that reported in [6].

Basing himself on results of compressive and flexural tests published in the literature, Hsu [7] established two equations for predicting the fatigue strength of concrete and verified their validity. One of these relates to fatigue in which failure occurs within 1000 load cycles, the other to fatigue with the number of cycles ranging from 10 to 10^7. The S-N curve calculated with the formulae (2) and (3) for $R = 0$ and $T = 0{,}120$ second is likewise given in Fig. 50.

As this curve is based on concentric (compressive) tests with no possibility of stress redistribution, the fatigue lives obtained are relatively shorter (see Section 4.1).

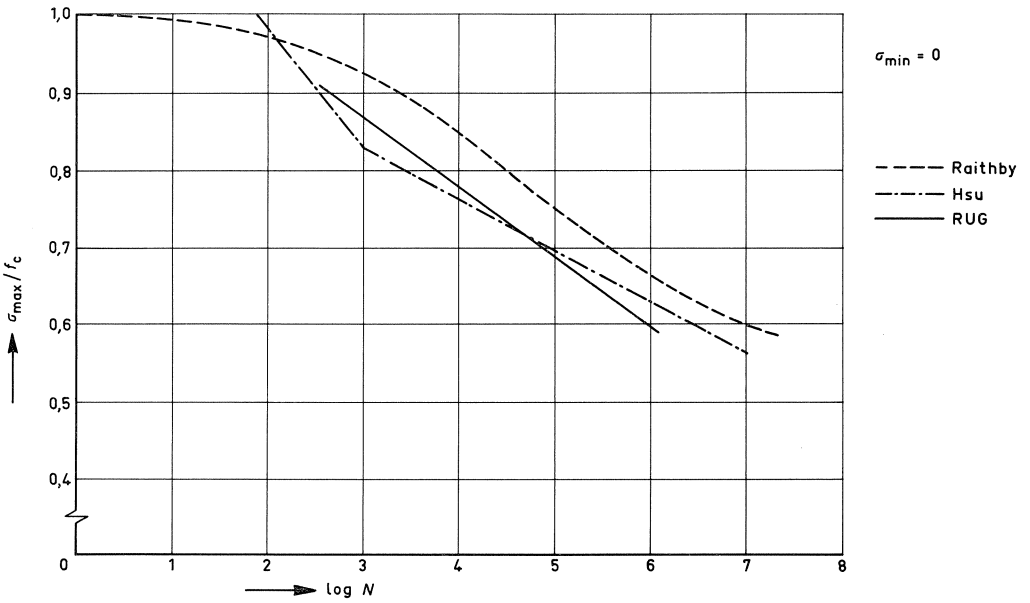

Fig. 50. Comparison of flexural tension results (RUG) with data published in the literature.

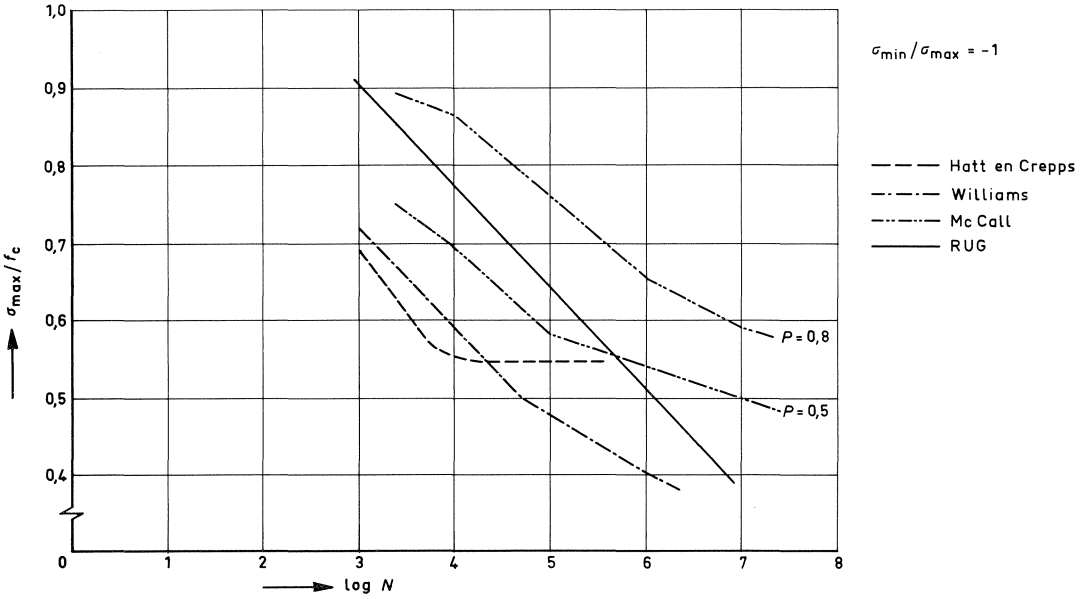

Fig. 51. Comparison of flexural tension results (RUG) with literature data for alternating tensile-compressive stresses.

Investigations in which test specimens were subjected to alternate tensile and compressive stresses of equal magnitude ("reversed loading") had earlier been performed by Hatt and Crepps [9, 10], Williams [11] and McCall [12]. The results of these investigations as well as those obtained by RUG are represented in the form of S-N curves for $\sigma_{min} = -\sigma_{max}$ in Fig. 51. The RUG curve was determined with the aid of the formulae (15) and (16) relating to the flexural tension research. With regard to comparing the results of RUG with those of McCall it should be noted that the former are represented as an average S-N curve which therefore corresponds to a failure probability $P = 0{,}5$. It appears that the results published in [9, 10, 11] distinctly lead to a lower number of cycles to failure, as contrasted with those published in [12]. A possible explanation for these differences may be sought in the very low frequency (0,166 – 0,25 Hz) applied in the three first-mentioned research projects as compared with the frequencies applied by RUG (8 Hz) and by McCall (30 Hz).

4.3 *Review of the results in a Goodman diagram*

The results of constant-amplitude tests can be summarized in a so-called Goodman diagram. Lines in this diagram each represent an equal number of cycles to failure. What combinations of upper and lower limit of the dynamic (fatigue) loading will lead to failure for any particular number of cycles can be deduced from the diagram.

In the upper part of the Goodman diagram in Fig. 52 the lines relate to the concentric tension and the flexural tension (and tension-compression) tests on "dry" concrete

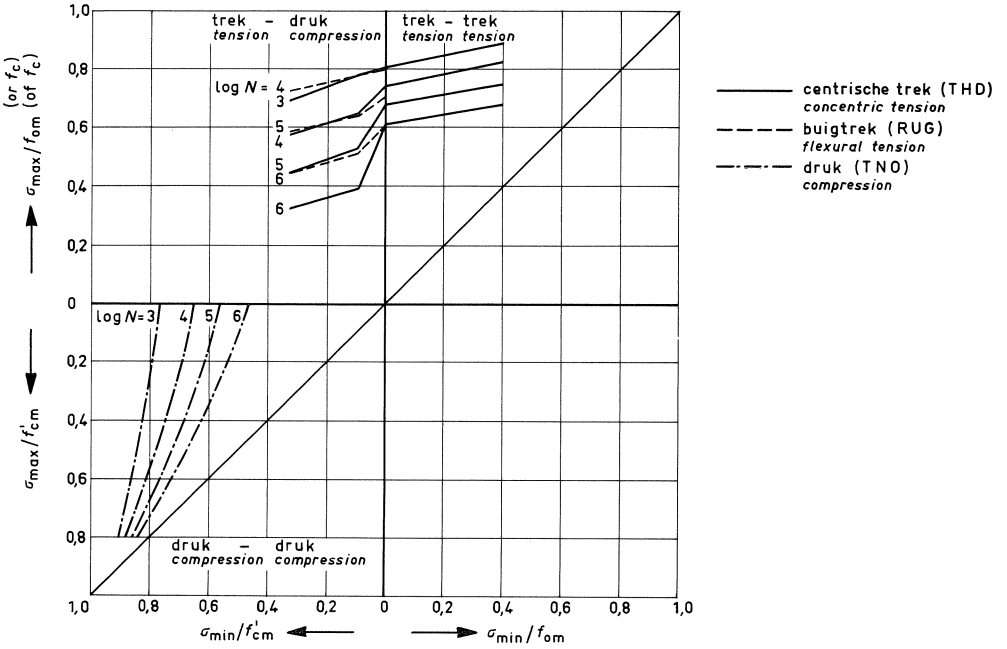

Fig. 52. Goodman diagram for tension, tension-compression and compression of concrete.

specimens. These lines represent average values and were calculated with the formulae (5) and (6) for concentric tension and (15) and (16) for flexural tension.

The lower part of the Goodman diagram contains the lines determined by TNO in tests on concrete loaded in compression [11].

Thus Fig. 52 presents an overview of the results of the constant-amplitude tests performed in the research conducted by the CUR-VB Committee C 33 "Alternating load".

By representing the results in a Goodman diagram it clearly emerges that the alternation of stress between tension and compression causes additional damage. For example, if the line for $\log N = 5$ in the upper of the diagram is considered, it is apparent that in the tension-tension region (on the right) a lowering of the lower limit must be associated with a proportionate lowering of the upper limit. But if the lower limit shifts to the compression region, the upper limit must decrease more than proportionately. This is particularly evident at the higher values of $\log N$.

This effect occurs in the uniaxial concentric tests as well as in the flexural tests, as the Goodman diagram shows.

A possible cause is the interaction of small cracks caused by tension in one direction and by compression in the direction perpendicular thereto.

The effect of stress alternation was further investigated in a supplementary series of tension-compression tests. In these the lower stress limits, in the compressive range, were chosen close to zero, namely, at 0, 2,5, 5 and 10% of the static compressive strength. The upper limits were at 60, 70 or 80% of the static tensile strength. The results

are given in Fig. 53. For a high upper limit ($0{,}8f_{om}$) a shift of the lower limit from 0 to a compressive stress has hardly any effect. For the lower values of the upper limit (0,7 and $0{,}6f_{om}$) there is a discontinuity, and distinctly fewer cycles to failure are attainable (a reduction from $\log N \cong 6$ to $\log N \cong 4$) if the stresses applied alternate between tension and compression.

The effect of the upper limit can be explained on the assumption that for an upper limit of $0{,}8f_{om}$ the cracking behaviour of the concrete is so dominated by this high tensile stress that interaction with small compressive cracks is of only minor importance. The alternation of the stress between tension and compression therefore adversely affects the fatigue life. In analogy with what has been said above, it must be expected that if the stress in a structure loaded predominantly in compression repeatedly turns into a tensile stress, the life of the structure will be reduced in consequence. This inference requires experimental verification, however.

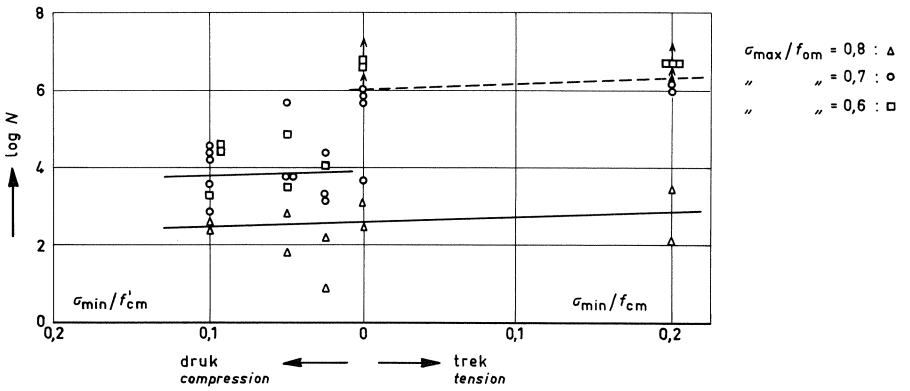

Fig. 53. Effect of the sign of the lower limit stress (tension or compression) on the number of cycles to failure.

5 Concentric program loading tests

5.1 *General*

To translate the resuls of constant-amplitude experiments into actual situation with complex loadings, Miner's rule is often aplied. According to this rule the damage contribution M due to a number of j cycles is the sum of the damage contributions of each individual cycle.

This rule can be expressed by the following equation:

$$M = \sum_{i=1}^{j} \frac{1}{N_i} \tag{16}$$

In this equation N_i is the number of cycles to failure in a constant-amplitude test with maximum and minimum levels according to cycle *i*. When the total damage becomes equal to unity it is presupposed that failure occurs. In the case of program loading tests

which consist of k successive blocks, each containing n_i equal loading cycles, equation (16) can be simplified to:

$$M = \frac{n_1}{N_1} + \frac{n_2}{N_2} + \ldots + \frac{n_k}{N_k} = \sum_{i=1}^{k} \frac{n_i}{N_i} \tag{17}$$

Although there are some fundamental objections to Miner's rule, no better rule is available at present. These objections concern the linearity, neglecting sequence effects, as well as the Miner number 1 at failure.

5.2 *Tests*

For concrete in repeated tension and in alternating tension-compression, Miner's rule was checked in program loading tests, in which specimens were subjected to a number of successive stress blocks characterized by minimum and maximum levels of the load cycles and a certain number of cycles per block (see Fig. 54).

The concentric tests were performed with specimens of the same shape as those, for the constant-amplitude tests. However, only sealed specimens were tested. The signal for the program loading was generated by a micro-computer. Eight different blocks having the same minimum stress could be generated. This set of blocks could be repeated. The transition from one block to the next took place at the minimum stress level. The measuring procedure was very similar to that of the constant-amplitude tests.

In order to check Miner's rule for concrete in tension, two block program loadings were first carried out. Sequence effects were studied by changing the sequence of high maximum stress blocks and lower maximum stress blocks.

The magnitude of the maximum stress levels was chosen in two regions: in a region with high stress levels ($\geqslant 0{,}70 f_{om}$) where cracking is predominant, and in a region with low stresses ($\leqslant 0{,}60 f_{om}$) were stress redistribution may be important [24]. During the tests the minimum stress level remained constant at values of $0{,}4 f_{om}$, $0{,}2 f_{om}$, 0,0, $0{,}05 f'_{cm}$ or $0{,}15 f'_{cm}$ respectively. These five lower levels were also applied in the continuation of the program loading tests with more than two blocks.

An overview of the different program loading tests is presented in Table 7 in which the number of cycles in each block is also indicated.

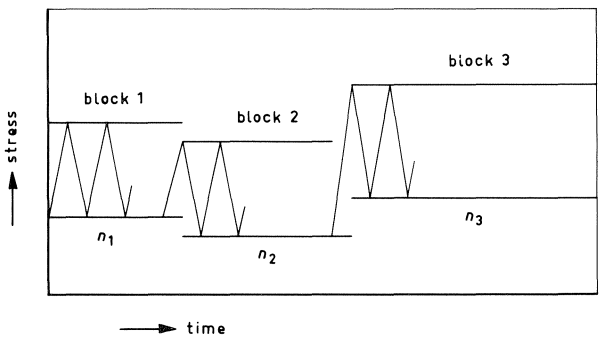

Fig. 54. General representation of program loading test.

Table 7. Summary of the investigated types of program loading tests

minimum stress-level	series 1	2	3	4	5	6
	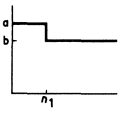	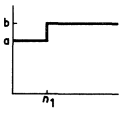	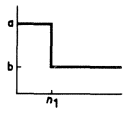	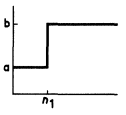	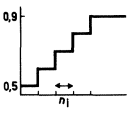	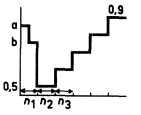
$0{,}15f'_{cm}$	$a = 0{,}75$*	0,70	0,70	0,40	0,50-0,90	$a = 0{,}75$
						$b = 0{,}70$
	$b = 0{,}70$	0,80	0,40	0,70		$n_1 = n_2 = 510$
	$n_1 = 510$	510	510	327600	$n_i = 4092$	$n_3 \ldots = 4092$
$0{,}05f'_{cm}$	$a = 0{,}75$	0,70	0,70	0,50	0,50-0,90	$a = 0{,}75$
						$b = 0{,}70$
	$b = 0{,}70$	0,80	0,50	0,80		$n_1 = n_2 = 510$
	$n_1 = 510$	510	510	327600	$n_i = 4092$	$n_3 \ldots = 4092$
0,00	$a = 0{,}80$	0,70	0,70	0,50	0,50-0,90	$a = 0{,}80$
						$b = 0{,}70$
	$b = 0{,}70$	0,80	0,50	0,80		$n_1 = 510$
	$n_1 = 510$	4092	510	327600	$n_i = 4092$	$n_2 \ldots = 4092$
$0{,}20f_{om}$	$a = 0{,}80$	0,70	0,70	0,50	0,50-0,90	$a = 0{,}80$
						$b = 0{,}75$
	$b = 0{,}75$	0,80	0,50	0,80		$n_1 = n_2 = 510$
	$n_1 = 510$	510	510	327600	$n_i = 4092$	$n_3 \ldots = 4092$
$0{,}40f_{om}$	$a = 0{,}80$	0,80	0,70	0,60	0,50-0,90	$a = 0{,}80$
						$b = 0{,}75$
	$b = 0{,}75$	0,90	0,60	0,90		$n_1 = n_2 = 510$
	$n_1 = 510$	510	510	327600	$n_i = 4092$	$n_3 \ldots = 4092$

* Fraction of static tensile strength

5.3 *Miner sums based on S-N diagrams*

According to equation (17) the Miner sums were calculated from 90 test results. The values of N_i were taken from the appropriate S-N equations (6) and (7) for "sealed" conditions. A summary of the Miner sums is given in table 8. In this table averages are also indicated. For the calculation of these average the run-outs were neglected.

It can be observed in the table that in general Miner sums exceeding unity were found. However, the results show considerable scatter, which complicates the analysis for estimating the effect of minimum stress level or series and also complicates a comparison with results from other investigations. These investigations concern concrete in compression and in bending [25, 26, 27]. It has been reported that if both blocks have high stress levels, Miner's rule satisfactorily describes damage. On the whole this finding is in accordance with our results in series 1 and 2. It has also been reported that it is favourable if a block has been preceded by a short block with high stresses.

This situation is met in series 3 where the Miner sums considerably exceeded $M = 1$ or could have exceeded this value if the tests had been continued.

Table 8. Miner sums based on S-N diagrams

minimum stress-level	series* 1	2	3	4	5	6	average
$0{,}15f'_{cm}$	1,04	5,46	> 3,40**	9,28	1,63	6,26	6,17
	3,48	1,02	> 3,40	6,09	0,44	43,77	
	1,65	4,71		4,49	4,53	1,86	
					3,05		
$0{,}05f'_{cm}$	7,42	13,09	> 11,48	6,85	13,99	1,94	9,24
	1,76	13,63	> 10,89	5,00	1,60	1,58	
	28,67	5,01		4,91	1,45	36,16	
						4,74	
0,00	> 71,03	10,68	> 0,44	8,16	95,24	5,45	17,07
	> 87,70	7,01	> 0,53	5,64	1,07	7,27	
	3,48	2,52		12,33	61,24	12,30	
	> 79,05					6,53	
$0{,}20f_{om}$	6,18	4,41	> 0,15	2,56	0,54	12,64	6,82
	1,79	0,64	> 0,15	1,07	61,46	3,09	
	1,30	1,68		0,19	7,18	1,63	
		2,71					
$0{,}40f_{om}$	0,55	2,42	> 0,96	4,69	0,46	9,96	3,16
	0,22	2,20	> 0,96	1,51	18,95	0,66	
	0,27	1,52		3,33	0,07	0,56	
average	4,45	4,92	-	5,07	17,05	9,20	

* See Table 7

** Denotes Miner sum is more, but test was stopped at 2×10^6 cycles (run-out)

However, generally considering the results in Table 8, no difference between series or between minimum levels can be ascertained. This is due to scatter which mainly originates from uncertainties in the stress-strength levels in the tests. For that reason the cyclic strains have also been evaluated, in order to correlate secondary strain rate and life in a particular stress block.

5.4 *Miner sums based on strain rate*

The cyclic strain was recorded during program loading tests. Two examples of the strains at maximum and minimum stress level are shown in Fig. 55 for a test with minimum stress level in tension and a test with minimum stress level in compression. With respect to the development of the peak strain, in each block a constant strain rate stage can be observed. As already explained in Section 3.2.3 (see "Theoretical models"), this strain rate can be used for estimating the number of cycles to failure more accurately than stress-strength level.

For estimating the number of cycles to failure under given loading conditions in a particular block, the relation with secondary strain rate was evaluated. In each block log $\dot{\varepsilon}_{sec}$ was determined (see Fig. 56); then with equation (12) log N was calculated, which

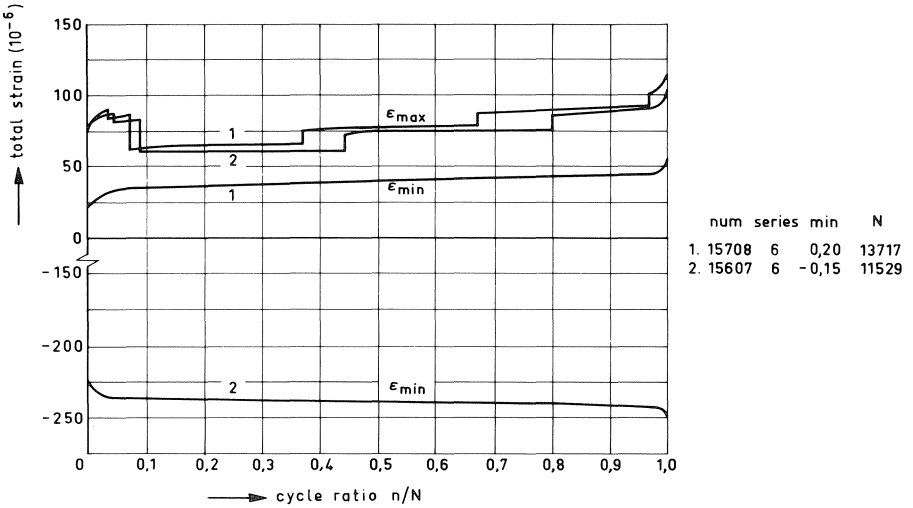

Fig. 55. Development of the strains at maximum and minimum of the cyclic stress in program loading tests.

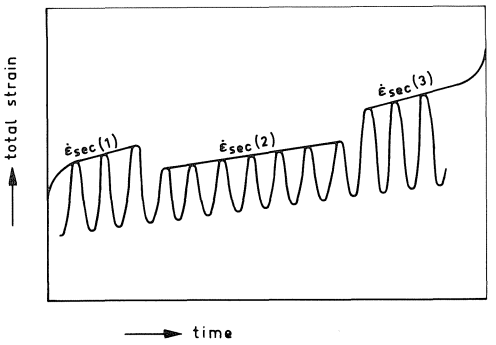

Fig. 56. Secondary strain rate in program loading tests.

was substituted into equation (17). The Miner sums are given in Table 9. Because of the extremely low $\dot{\epsilon}_{sec}$ in the second block of series 3, no Miner sums are given there.

As appears from Table 9, there is little scatter in the results. As pointed out before, this is so because the actual stress level of the specimen is taken into account. Also, in general, the Miner sums are smaller than in Table 8. One reason for this is that the effect of the preceding blocks is expressed in the slope of cyclic peak strain in the block that is considered. So the damaging effect of the preceding load cycles is taken into account. It can be concluded from the table that in general Miner sums in excess of unity have been found and that the minimum level and sequence of the blocks have little influence in this calculation procedure. Miner's rule could successfully be applied and the failure criterion $M = 1$ proved to be safe in general.

The practical significance of the evaluation of secondary strain rate is that a more

Table 9. Miner sums based on secondary creep rate

minimum stress-level	series* 1	2	4	5	6	average
$0{,}15f'_{cm}$	0,64	0,86	0,76	0,57	1,53	0,92
	1,12	0,51	1,00	0,46	1,18	
	0,65	0,91	0,39	1,66	1,02	
				1,53		
$0{,}05f'_{cm}$	1,16	1,39	0,41	1,16	0,68	1,05
	0,90	0,92	0,83	1,39	0,86	
	0,94	1,73	0,87	1,16	1,21	
					1,12	
0,00	> 2,38**	1,60	1,19	2,01	1,16	1,86
	> 2,02	1,72	2,20	1,74	2,38	
	1,56	1,22	1,84	2,33	2,53	
	> 3,00				2,07	
$0{,}20f_{om}$	2,72	2,38	1,79	1,59	2,18	1,83
	1,31	1,84	1,41	2,33	2,16	
	1,44	1,09	0,65	2,77	2,04	
		1,53				
$0{,}40f_{om}$	3,13	4,17	1,59	2,80	2,75	2,13
	1,29	1,59	0,68	2,91	2,17	
	1,56	1,48	1,01	2,35	2,51	
average	1,42	1,59	1,11	1,80	1,77	

* See Table 7

** Denotes Miner sum is more, but test was stopped at $0{,}5 \times 10^6$ cycles

accurate estimation of fatigue life can be established, as has also been shown by Sparks [29]. Uncertainties in concrete strength such as occur in practice can be taken into account by referring the cyclic stresses to the characteristic strength values.

A more direct application of a calculation procedure based upon secondary strain rate, however, requires further research with respect to its dependence on various important influential factors.

6 Summary and conclusions

The subject of this research is the fatigue behaviour of plain (unreinforced) concrete under tensile and under tensile-compressive stresses. Such stress conditions are important because they may exercise an influence on the cracking behaviour and thus, inter alia, on the stiffness and the damping of structures. The cracking behaviour is moreover of influence on the bond of reinforcing steel and on durability.

The fatigue tests were carried out by two methods. In the Stevin Laboratory of the Delft University of Technology (THD) the tests were performed with uniaxial concentric loading, while those performed in the Magnel Laboratory of the State University of Ghent (RUG) in Belgium consisted of three-points bending tests. In order to achieve

mutual comparability of the results, the experimental conditions, such as concrete mix composition and age at testing, were interadjusted as much as possible.

The experimental research began with constant-amplitudes tests. The object was, primarily, to determine the number of cycles to failure as a function of the limits between which the load signal varied in order thus to determine S-N diagrams for concrete loaded in tension. These limits were so chosen that the maximum in all cases was a tensile stress and that the minimum was a tensile, a zero of a compressive stress. This compressive stress in no case exceeded 30% of the compressive strength, so that failure always occurred as a result of the tensile strength being exceeded.

Only one mix composition, producing concrete of strength class B 45, was used in the research program. The frequency of the sinusoidal load signal was 6 Hz (THD) and 8 Hz (RUG). In the THD tests the moisture conditions of the specimens were either wet or dry, while in the RUG tests the specimens were always tested in the dry condition. In both laboratories the fatigue tests were performed in the fifth week after the specimens had been cast.

Cylindrical tests specimens (120 mm diameter, 300 mm height) with somewhat enlarged end faces were used in the uniaxial concentric loading tests. These specimens were cast 12 at a time. About six of them were used for determining the static tensile strength and the others were used for fatigue testing. The specimens for bending tests were beams with dimensions of 150 mm × 280 mm × 2300 mm. The flexural strength (modulus of rupture) was first determined on one half of such a beam. Then the fatigue test was performed on the other half. A compressive stress was maintained in the bottom fibre by means of prestressing. In the fatigue tests the tensile stresses were always related to the static strength values, namely, the flexural strength or the concentric (direct) tensile strength. The compressive stresses were expressed as percentages of the cube (compressive) strength.

The results of the fatigue tests are represented in S-N diagrams. The regression lines for the relation between the fatigue life attained and the stresses applied were also determined.

From the results it emerges that the life (the number of cycles to failure) is strongly dependent on the maximum tensile stress of the sinusoidal signal. The larger this stress, the shorter the life.

Also, shorter values for the life were found when, for a given upper limit, the lower limit was lowered. This was more particularly the case when, as a result of such lowering, the stress alternated from tension to compression. It furthermore emerged from the tests that the number of cycles to failure was lower for wet specimens than for dry ones.

In the uniaxial concentric tests performed at Delft (THD) the longitudinal strain was measured during the fatigue tests. This strain was brought into relation with internal cracking (damage).

From the analysis of the strains it was deduced that both the rate of strain and the magnitude of the strain are factors determining the life attained by the specimen. It is possible to make an accurate estimate of the number of cycles to failure from the rate of strain.

On comparing the results of the bending tests (RUG) and those of the uniaxial concentric tests (THD) it was found that, for equal load signals applied, longer lives were attained in the first-mentioned tests. This is attributable to scatter in the strength values and to the possibility of stress redistribution due to the presence of a stress gradient in the bending tests.

In order to simulate practical loading conditions and to investigate whether Miner's rule can suitably be applied to concrete loaded in tension, the experimental research was continued with program loading tests. These were concentric uniaxial tests performed at the Delft University of Technology (THD). They comprised two- and multi-block tests. Mainly in consequence of the scatter in the strength properties of the specimens the Miner sum likewise showed considerable scatter. However, if the Miner sum was calculated on the basis of strain rate, not stress, the scatter was reduced. In this way it was established that Miner's rule is applicable and that the failure criterion $M = 1$ is, in general, a safe approximation.

The following general conclusions can be reported:

- Stress reversals (change of sign, i.e., tension-compression) lead to additional damage and therefore shorten the fatigue life.
- Because of the possibility of redistribution of stresses, a stress gradient has a favourable effect on the length of life.
- Scatter in the number of cycles to failure is strongly influenced by variations in the static strength.
- Miner's rule can be applied to estimate fatigue life of concrete subjected to repeated tensile or alternating tensile-compressive stresses, especially if partial damage is deduced from secondary strain rate. Program loading tests indicate that $M = 1$ is a safe criterion in general.

The fatigue research at the Delft University of Technology (THD) is to be continued within the framework of the Marine Technological Research (MaTS) project. The effect of randomly varying loads, such as occur in practice, is under investigation. Also it is intended to complete the Goodman diagram for combination of high compressive and low tensile stresses. Furthermore, it is being endeavoured to develop a physical model for the fatigue of concrete.

7 Notation

a	edge length of cube	mm
e	eccentricity	mm
f_b	splitting tensile strength	N/mm^2
f_c	flexural (tensile) strength	N/mm^2
f_0	direct (concentric) tensile strength	N/mm^2
f_c'	cube (compressive) strength	N/mm^2
i_m	mean (on average) value of the quantity i	
k, m	coefficients	
n	cycle	

v	deformation	mm
$V(i)$	coefficient of variation of the quantity i	%
w	crack width	mm
A	cross-sectional area	mm^2
D	measure of destruction	
E_b	modulus of elasticity of concrete in tension	N/mm^2
E'_b	modulus of elasticity of concrete in compression	N/mm^2
F	load	N
F_{max}	maximum load	N
F_{min}	minimum load	N
M	Miner sum	
N	number of cycles to failure	
$P\{x\}$	probability of a particular event x	%
R	$\sigma_{min}/\sigma_{max}$	
T	period	s
ε_1	strain associated with minimum tensile stress	
ε_e	elastic strain	
ε_{tot}	total strain	
$\dot{\varepsilon}_{sec}$	secondary creep rate	per s
φ_{cycl}	cyclic creep coefficient	
σ_b	splitting tensile stress	N/mm^2
σ_{max}	maximum stress	N/mm^2
σ_{min}	minimum stress	N/mm^2

8 Reference

1. CUR-VB rapport 112, Vermoeiing van beton, deel 1: drukspanningen.
2. Domone P. L., Uniaxial tensile creep and failure of concrete. Magazin of concrete Research, Vol. 26 No. 88, September 1974.
3. Heilmann, H. G., Zugspannung und Dehnung in unbewehrten Betonquerschnitten bei exzentrischer Belastung. DAF Stb. Heft 269, Berlin, 1976.
4. Kolias, S. en R. I. T. Williams, Cement-bound road materials: strength and elastic properties measured in the laboratory. TRRL Report No. 344, 1978.
5. Morris, A. D. en G. G. Garrett, A comparative study of the static and fatigue behaviour of plain and steel fibre reinforced mortar in compression and direct tension. International Journal of Cement Composites and Lightweight concrete, Vol. 3 No. 2, May 1981.
6. Raithby, K. D., Some flexural fatigue properties of concrete-effects of age and methods of curing. First Australian Conference on Engineering Materials, University of New South Wales, 1974.
7. Hsu, T. C., Fatigue of plain concrete. ACI Journal, Proceedings Vol. 78, July/August 1981.
8. Rusch, H., Researches toward a general flexural theory for structural concrete, ACI Journal, Proceedings Vol. 57, No. 1, July 1960.
9. Hatt, W. K., Fatigue of concrete. Proceedings, Highway Research Board, N. 4, December 1924.
10. Crepps, R. B., Fatigue of mortar. Proceedings, ASTM, Vol. 23, Part II, 1922.
11. Williams, H. A., Fatigue tests of lightweight aggregate concrete beams. ACI Journal. Proceedings Vol. 39, No. 5, April 1943.

12. McCall, J. T., Probability of fatigue of plain concrete. ACI Journal, Proceedings Vol. 55, No. 2, August 1958.
13. Linger, D. A. en H. A. Gillespie, A study of the mechanism of concrete fatigue and fracture HRB Research News, No. 22, February 1966.
14. Tepfers, R., Tensile fatigue strength of plain concrete. ACI Journal, August 1979.
15. Tepfers, R., Fatigue of plain concrete subjected to stress reversals. ACI special publication 75, 1982.
16. Cornelissen, H. A. W. en G. Timmers, Fatigue of plain concrete in uniaxial tension and in alternating tension-compression loading. Report No. 5-81-7, Stevin Laboratory, Delft University of Technology, 1981.
17. Cornelissen H. A. W. en H. W. Reinhardt, Fatigue of plain concrete in uniaxial tension and in alternating tension-compression loading. Proceedings IABSE-colloquium Lausanne, 1982.
18. Siemes, A. J. M. en H. A. W. Cornelissen, Vermoeiing van ongewapend beton. Cement No. 8, 1982.
19. Wittmann, F. H. en Y. V. Zaitsev, Verformung und Bruchvorgang poröser Baustoffe bei kurzzeitiger Belastung und Dauerlast. DAFstb Heft 232, 1974.
20. Vermoeiing van beton - Deel 2: Vermoeiing aan trek- en trek-drukwisselingen. Test Report No. 78/737, Magnel Laboratory for Reinforced concrete, State University of Ghent, Belgium, December 1979.
21. Vermoeiing van beton aan trek-drukwisselingen. Research Report 81/001, Magnel Laboratory for Reinforced concrete, State University of Ghent, Beldium, December 1981.
22. Ople, F. S. en C. L. Hulsbos, Probable fatigue life of plain concrete with stress gradient. Journal of the ACI proceedings 63/1966.
23. Dillmann, R. R., Die Spannungsverteilung in der Biegedruckzone von Stahlbetonquerschnitten bei häufig wiederholter Belastung. PhD thesis TH. Darmstadt, 1981.
24. Shah, S. P. and S. Chandra, Fracture of concrete subjected to cyclic and sustained loading, Report 69-4 Dept. of Mat. Engineering, University of Illinois of Chicago Circle, June 1969.
25. Holmen, J. O., Fatigue of concrete by constant- and variable-amplitude loading, ACI-SP-75, 1982, pp. 71-110.
26. Weigler, H., Beton bei häufig wiederholter Beanspruchung, Beton Vol. 31, No. 5, 1981, pp. 189-194.
27. Hilsdorf, H. K. and C. E. Kesler, Fatigue strength of concrete under varying flexural stresses, ACI Journal, Proc. 63, 1966, pp. 1059-1076.
28. Sparks, P. R., The influence of rate of loading and material variability on the fatigue characteristics of concrete, ACI, SP-75, pp. 331-341.

APPENDIX A

Review of static strengths for concentric tensile tests

Table A1. Results of the static tests for concentric tensile testing

batch No.	f'_{cm} (N/mm^2)	$V(f'_c)$ (%)	f_{bm} (N/mm^2)	$V(f_b)$ (%)	f_{om} (N/mm^2)	$V(f_0)$ (%)	E_{bm} (N/mm^2)	$V(E_b)$ (%)	ε_{1m} (10^{-6})	$V(\varepsilon_1)$ (%)
17	45,07	3,6	2,99	6,3	2,39	5,1				
18	45,69	10,9	2,89	2,4	2,07	7,2				
20	46,96	4,7	2,82	6,1	2,35	5,9				
21	47,24	5,8	3,39	9,8	2,03	9,7				
22	48,96	6,1	3,32	9,7	2,37	6,7				
23	50,83	3,4	2,90	11,7	2,09	9,9	not measured			
24	46,86	8,7	2,96	8,8	2,20	10,0				
25	51,20	4,1	2,98	9,8	2,40	6,1				
26	48,81	1,9	2,76	12,9	2,12	7,8				
27	49,18	1,7	2,94	1,2	2,36	12,6				
28	50,86	3,4	3,00	2,3	2,45	7,1				
29	48,02	2,3	2,91	14,4	2,38	6,9				
30	45,60	20,8	2,86	12,4	2,52	5,9				
31	47,18	5,9	3,25	5,1	2,40	7,9				
32	46,24	4,6	3,51	6,8	2,48	9,8				
33	48,82	4,0	3,01	4,5	2,41	8,3				
34	49,24	3,4	3,00	9,6	2,54	9,0				
35	46,73	2,9	2,82	8,5	2,42	8,8				
36	49,08	1,6	2,43	9,6	2,59	9,6				
37	48,12	2,2	2,53	10,1	2,35	7,4				
38	47,11	2,2	2,45	8,8	2,57	5,3				
59	47,41	8,4	3,19	7,2	2,45	8,3				
60	53,03	5,3	2,94	7,4	2,63	3,5				
61	49,34	1,6	3,14	4,5	2,74	2,8				
62	50,72	1,5	2,93	3,9	2,55	4,5				
64	49,08	8,1	3,87	12,7	2,56	9,8				
65	51,51	3,9	3,22	5,9	2,57	8,1	34570	7,9	106	9,1
67	47,18	3,3	2,87	4,5	2,72	3,8	34810	7,1	104	7,2
68	43,62	0,6	3,07	1,9	2,56	5,5	34660	6,7	96	7,0
71	47,27	0,5	2,59	12,1	2,52	7,3	33410	1,9	105	12,4
72	50,28	2,3	2,88	3,2	2,60	4,8	34010	1,2	109	5,2
73	45,85	1,9	2,36	7,0	2,39	8,0	39020	21,4	87	10,4
74*	42,47	2,1	2,40	11,5	2,75	1,9	35590	6,0	117	3,0
75*	46,07	2,1	2,86	13,2	2,92	4,6	37880	12,1	124	10,7
76*	46,90	3,1	2,81	11,4	2,72	4,2	36010	3,4	116	6,4
77*	45,52	0,8	2,84	6,6	-	-	-	-	-	-
78*	44,29	1,5	2,25	1,0	-	-	-	-	-	-
79*	43,67	1,9	2,52	5,4	2,73	5,2	32280	7,4	130	11,2
80*	44,68	2,4	2,62	9,6	2,93	3,6	34620	8,1	133	6,8
81*	43,49	3,9	2,21	4,6	2,78	5,1	34080	6,0	126	12,9
82*	45,85	5,4	2,39	6,1	2,80	3,2	38820	18,2	118	8,9

Table A1. (continued)

batch No.	f'_{cm} (N/mm^2)	$V(f'_c)$ (%)	f_{bm} (N/mm^2)	$V(f_b)$ (%)	f_{om} (N/mm^2)	$V(f_0)$ (%)	E_{bm} (N/mm^2)	$V(E_b)$ (%)	ε_{1m} (10^{-6})	$V(\varepsilon_1)$ (%)
83*	43,26	2,2	2,30	7,7	2,78	3,5	35170	8,1	126	10,2
84*	45,54	7,1	2,44	7,0	2,69	2,2	34050	5,9	121	5,8
85	44,49	4,8	2,46	8,2	2,55	6,7	38340	5,5	90	5,5
86	47,51	1,8	2,71	8,0	2,29	6,6	35260	5,7	95	11,8
87	51,73	3,8	2,49	13,7	2,30	7,2	33930	3,3	89	8,1
88	50,52	3,6	2,98	7,7	2,49	5,9	36200	14,0	91	7,9
89	47,27	2,9	2,78	0,6	2,62	8,4	37140	5,2	93	8,7
90	50,34	0,6	2,92	5,3	2,37	6,3	37340	14,2	90	9,3
91	50,14	2,2	3,09	8,7	2,64	6,3	37580	1,5	97	8,2
95	47,13	2,9	2,84	10,2	2,93	3,7	-	-	-	-
96	49,07	2,9	3,15	3,7	2,73	4,3	-	-	-	-
97	50,47	1,7	3,09	3,6	2,73	9,4	34230	2,2	113	9,9
98	47,80	7,4	2,93	6,9	2,63	4,7	33080	2,4	110	7,2
99*	46,17	4,1	3,43	10,7	2,97	5,1	33550	3,7	144	13,0
100*	44,40	3,3	3,11	3,6	2,92	5,2	-	-	-	-
101*	44,60	4,7	3,27	4,6	3,01	1,0	-	-	-	-
102*	41,07	3,3	3,23	2,7	2,94	3,5	-	-	-	-
103*	45,67	1,7	2,83	10,8	3,12	2,1	36400	5,1	125	1,3
104*	46,25	1,4	2,94	5,8	3,18	2,0	35840	3,5	125	4,3
105*	42,63	5,4	2,68	1,1	3,07	1,8	35780	3,6	128	7,3
106*	-	-	-	-	3,04	1,2	35710	2,6	126	8,0
107*	48,43	2,7	2,96	1,0	3,07	3,1	36330	2,4	120	6,1
108*	48,03	5,7	2,98	7,2	2,92	1,6	37940	1,6	112	1,6
109	44,07	6,2	3,00	10,9	2,82	6,6	43040	2,8	88	10,4
110	49,03	3,4	2,80	7,3	2,44	13,5	37550	3,6	91	16,8
111	50,63	6,6	3,09	5,8	2,36	2,7	38310	2.3	90	4,0
112	46,67	3,0	3,19	5,2	2,54	15,6	36570	7,6	93	9,0
114	47,67	1,0	2,69	11,8	2,40	11,5	35830	4,9	99	14,1
115	48,10	4,5	2,87	7,0	2,45	8,3	37360	3,0	89	7,9
116	48,17	2,8	2,97	9,7	2,29	2,4	36910	1,9	84	6,2
117	48,83	4,4	2,84	2,0	2,30	13,0	35320	2,4	89	10,5
118	47,20	3,9	2,93	6,1	1,86	18,0	35500	2,5	80	17,4
119	49,10	5,1	2,63	6,9	2,58	3,1	35000	3,3	103	10,0
120	47,20	3,6	2,63	3,5	2,50	11,4	34630	1,7	103	14,5
121*	45,92	3,2	2,55	3,9	3,06	6,9	35100	1,3	137	7,8
122*	46,16	2,1	2,62	1,8	2,80	9,9	34950	4,3	115	13,4
123*	47,88	3,5	2,80	9,9	3,12	3,8	34680	3,8	130	6,6
aver-age	47,34	3,8	2,87	7,0	2,46 2,92*	7,6 3,7*	36140 35515*	5,2 5,6*	96 125*	9,6 7,7*

* = wet

APPENDIX B

S-N diagrams for concentric tensile tests (6 Hz)

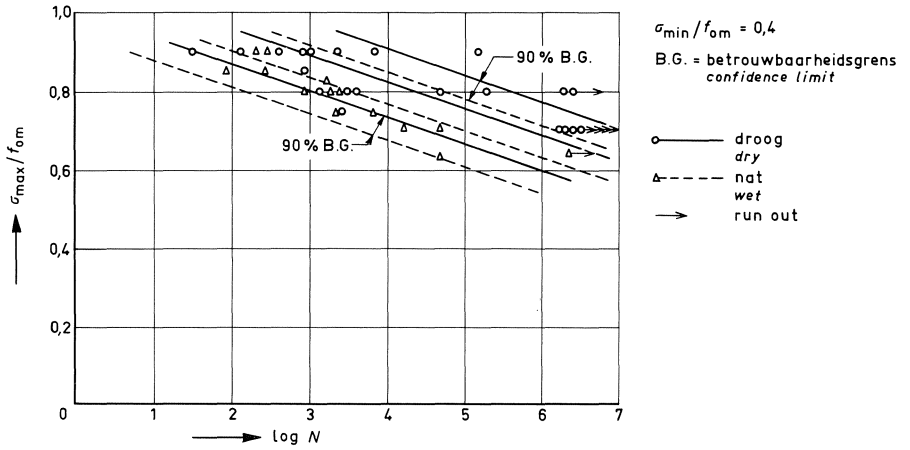

Fig. B1. S-N diagram for pulsating tensile tests.

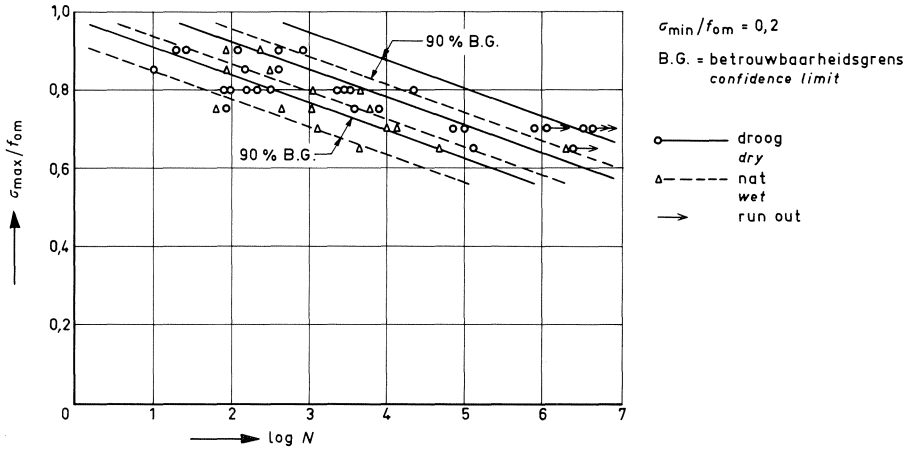

Fig. B2. S-N diagram for pulsating tensile tests.

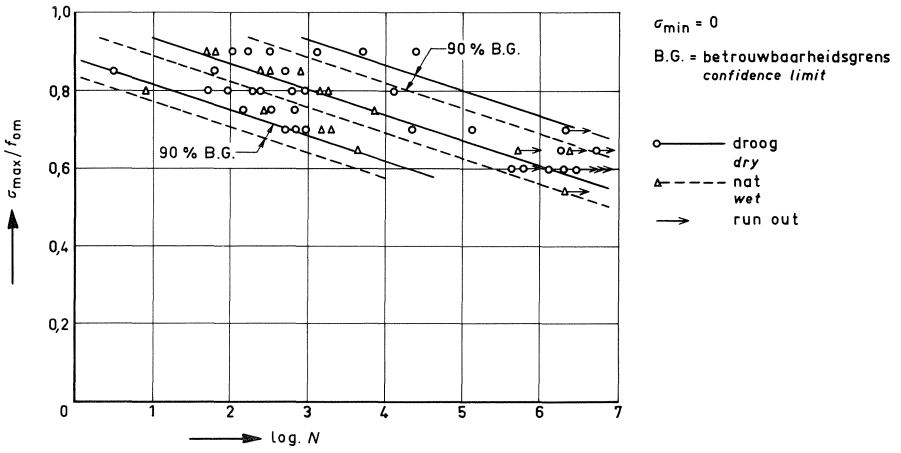

Fig. B3. S-N diagram for pulsating tensile tests.

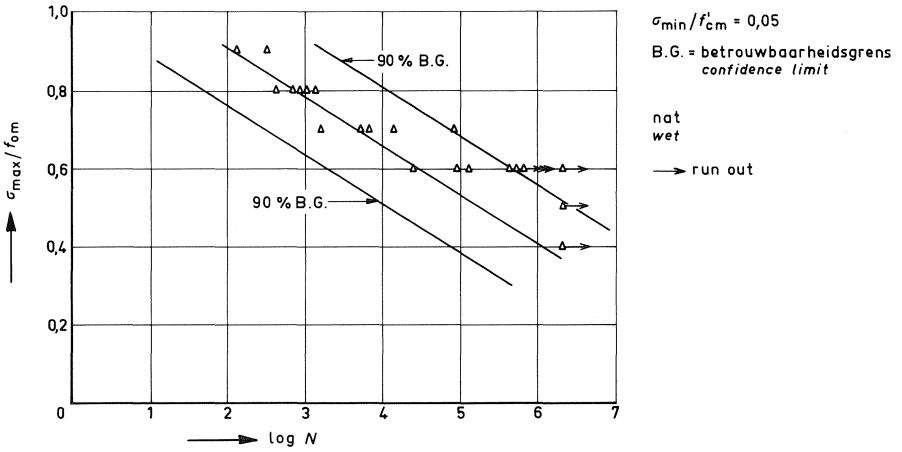

Fig. B4. S-N diagram for alternating tensile-compressive tests.

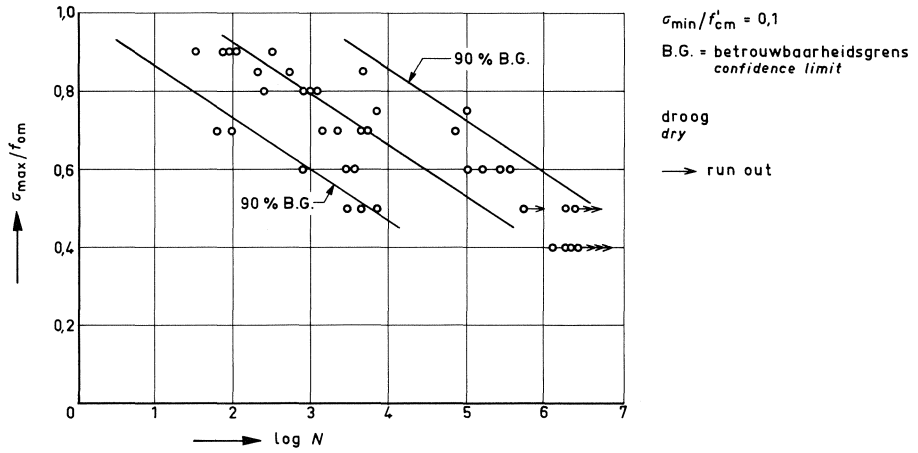

Fig. B5. S-N diagram for alternating tensile-compressive tests.

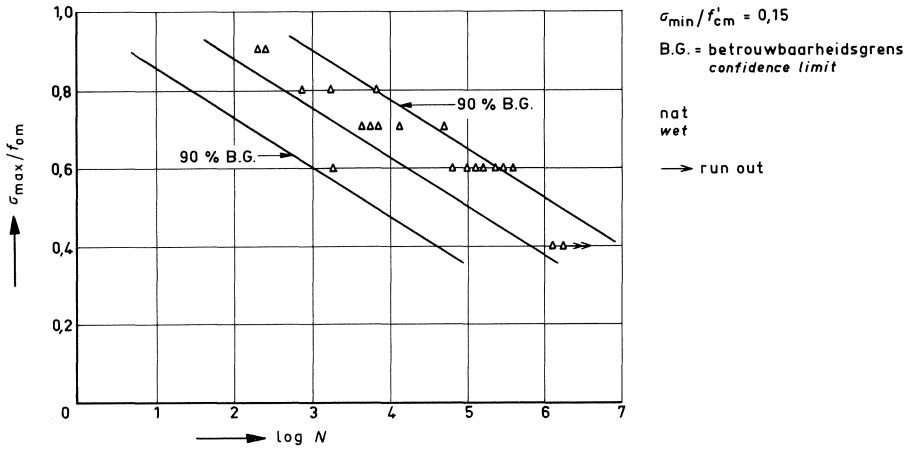

Fig. B6. S-N diagram for alternating tensile-compressive tests.

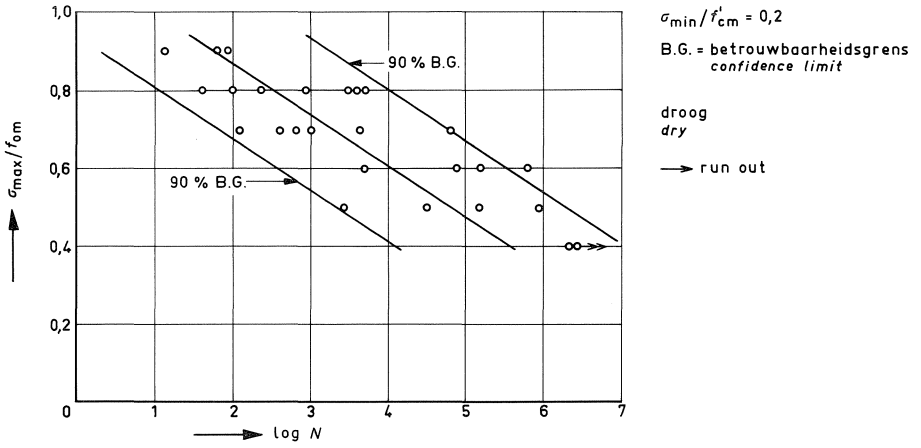

Fig. B7. S-N diagram for alternating tensile-compressive tests.

APPENDIX C

S-N diagrams of concentric tensile tests (0,06 Hz)

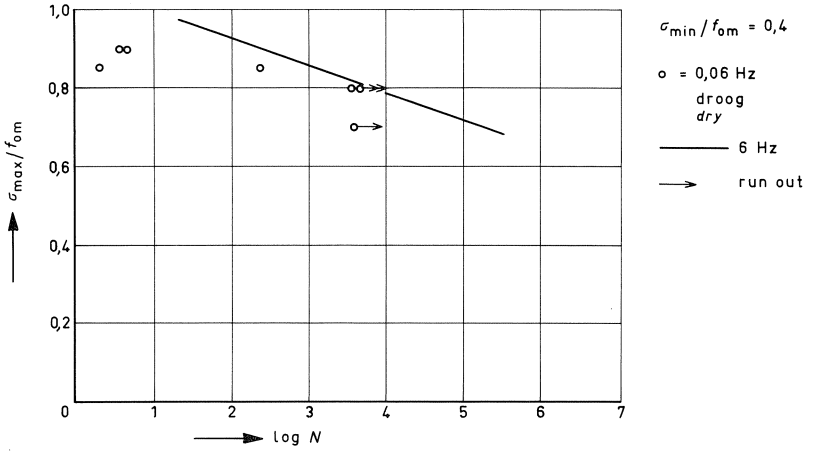

Fig. C1. Measured points obtained in pulsating tensile tests at 0,06 Hz.

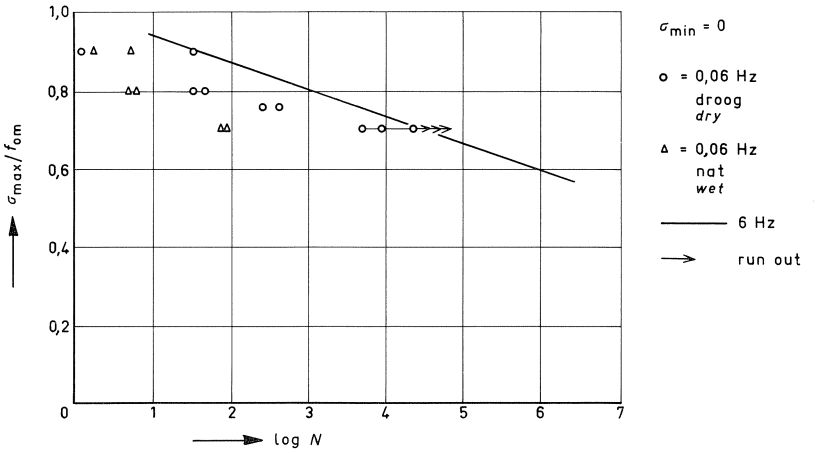

Fig. C2. Measured points obtained in pulsating tensile tests at 0,06 Hz.

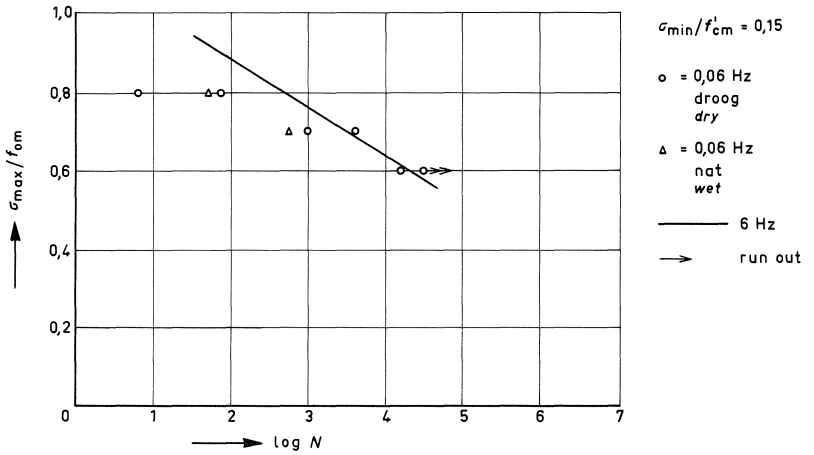

Fig. C3. Measured points obtained in pulsating tensile tests at 0,06 Hz.

APPENDIX D

Crack detection in fatigue tests

If cracking of the concrete occurs during a fatigue test, a specially designed switching circuit causes the pulsator to stop (and therefore also stops the cycle counter). For this purpose four electrical resistance strain gauges (type KYOWA KC 70) with 68 mm gauge length are affixed - at the load position - to the underside of the test specimen (see Fig. D1). These gauges are connected in a full bridge arrangement and form part of an electrical switching circuit comprising the following components:

- amplifier unit;
- comparator (for setting two limit values);
- relay control system;
- oscilloscope.

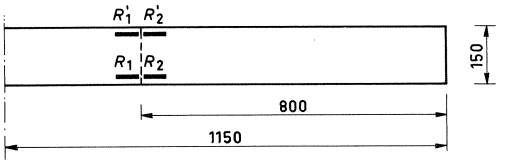

Fig. D1. Position of electrical resistance strain gauges on the underside of the specimen.

The principle of the crack detection procedure is illustrated by the block diagram in Fig. D2:

- the formation of a fatigue crack in a dynamically loaded prestressed specimen disturbs the equilibrium of the Wheatstone bridge and causes the comparator to respond when the two preset limit values are exceeded;
- the amplified signal is then fed to a relay which operates the energizing circuit of the pulsator and causes the latter to be switched off.

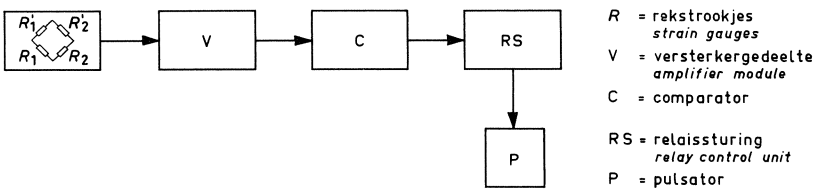

Fig. D2. Block diagram of the crack detection system.

APPENDIX E

Review of static strengths for flexural tensile tests

Table E1. Flexural strength (f_c) of the specimens for the fatigue tests.

specimen No.	flexural strength f_c (N/mm^2)	specimen No.	flexural strength f_c (N/mm^2)	specimen No.	flexural strength f_c (N/mm^2)
1-39*	4,70	36-28	4,10	57-16	4,45
2-19	4,40	37-17	3,70	58-39	3,95
3-29	4,20	38-29	3,85	58-27	4,00
4-09	3,90	39-16	3,75	59-17	4,55
5-38	4,75	40-29	3,80	59-06	4,35
6-18	4,75	41-24	4,20	60-37	4,05
7-28	4,60	42-34	4,30	60-26	4,15
8-08	4,55	43-18	4,55	61-08	4,70
9-37	4,05	43-07	4,40	61-15	3,95
10-17	4,60	44-28	4,45	62-37	4,40
11-27	4,00	44-37	4,30	62-36	4,15
12-07	4,25	45-09	5,00	63-07	4,50
13-36	4,20	45-16	4,50	63-06	5,00
14-16	4,10	46-25	4,35	64-38	4,50
15-26	3,70	47-19	5,05	64-25	4,30
16-06	3,95	47-08	4,50	65-07	4,00
17-35	3,80	48-29	4,65	65-15	4,70
18-15	3,90	48-36	4,65	66-08	3,90
19-25	4,15	49-09	4,45	66-15	4,85
20-07	4,20	49-17	3,80	67-09	4,75
21-29	4,75	50-39	4,25	67-14	4,15
22-19	4,50	50-25	4,55	68-39	4,60
23-28	4,10	51-18	4,40	68-24	4,50
24-09	4,55	51-06	4,50	69-38	4,90
25-28	4,15	52-38	4,40	69-35	4,95
26-18	4,45	52-28	3,95	70-07	3,40
27-08	4,55	53-19	3,95	70-05	4,50
28-27	4,50	53-09	4,25	71-26	5,00
29-17	4,40	54-29	5,15	71-34	4,00
30-26	4,25	54-36	4,60	72-26	4,50
31-07	4,00	55-19	4,15	72-35	3,70
32-25	4,00	55-08	4,30	73-09	3,95
33-18	3,80	56-27	4,70	73-04	3,90
34-25	4,20	56-35	4,05	74-07	4,00
35-16	4,00	57-08	4,00	74-06	4,55

average: 4,30 N/mm^2
coefficient of variation: 8,1%

* 1-39 ← $\sigma_{max} = 0{,}9\, f_c$
batch No. ↑ $\sigma_{min} = 0{,}3\, f'_{cm}$

Table E2. Results of the static tests for flexural tensile testing

batch No.	compressive strength f'_{cm}* (N/mm^2) cube $200 \times 200 \times 200$ mm^3	flexural strength f_{cm}* (N/mm^2) prism $150 \times 150 \times 600$ mm^3	secant modulus of elasticity E'_b** (N/mm^2) prism $200 \times 200 \times 500$ mm^3
1	47,2	4,15	36300
2	48,4	4,30	35200
3	48,4	4,45	36100
4	48,6	3,80	34400
5	51,0	4,30	35000
6	49,4	4,20	37700
7	48,4	4,05	37500
8	51,4	4,05	35500
9	50,0	4,05	36300
10	51,6	4,50	34500
11	50,8	4,70	35200
12	47,8	4,40	37200
13	49,6	4,20	36100
14	48,6	4,00	36000
15	51,0	4,10	37400
16	51,2	4,05	34400
17	46,8	4,50	38700
18	47,6	4,40	35100
19	50,4	4,50	35800
20	51,0	4,20	35700
21	50,4	4,75	37800
22	49,6	4,40	37400
23	49,2	4,25	36100
24	48,6	4,25	37100
25	49,0	4,10	38200
26	54,2	4,10	37500
27	52,2	4,45	35900
28	51,6	4,40	36700
29	50,0	4,10	35000
30	48,4	4,10	35700
31	49,2	4,45	35300
32	46,0	4,00	38300
33	48,2	4,35	38100
34	49,0	3,95	37500
35	50,8	4,30	36900
36	49,2	3,85	36400

* average of three specimens per batch
** E'_b determined for one prism per batch

Table E2. (continued)

batch No.	compressive strength f'_{cm}* (N/mm^2) cube 200 × 200 × 200 mm^3	flexural strength f_{cm}* (N/mm^2) prism 150 × 150 × 600 mm^3	secant modulus of elasticity E'_b** (N/mm^2) prism 200 × 200 × 500 mm^3
37	47,0	3,75	38300
38	47,0	3,75	33500
39	51,4	4,05	34600
40	50,0	3,70	35000
41	49,2	4,15	36600
42	51,2	4,10	37500
43	52,6	4,85	35600
44	49,6	4,85	37900
45	53,8	5,20	37700
46	56,8	4,60	37100
47	52,2	5,00	37900
48	49,8	4,95	35900
49	48,4	4,40	36100
50	47,6	4,55	37800
51	46,4	4,50	34900
52	46,0	4,65	36400
53	49,4	4,85	37100
54	50,8	5,20	38100
55	49,8	5,20	36200
56	47,4	4,90	36600
57	49,0	4,45	35800
58	48,4	4,30	36000
59	47,8	4,55	36900
60	46,6	4,20	35500
61	46,6	4,90	35500
62	47,6	4,45	36500
63	47,6	4,75	37400
64	51,6	5,05	35800
65	48,8	4,95	36100
66	49,4	4,60	35400
67	47,6	4,40	35000
68	48,8	4,65	35700
69	49,4	4,85	35500
70	47,6	4,05	35600
71	46,8	4,20	37300
72	45,6	4,10	37000
73	46,4	3,95	35400
74	44,4	4,25	37600
average	49,2 N/mm^2	4,40 N/mm^2	36300 N/mm^2
coefficient of variation	4,3%	8,3%	3,3%

* average of three specimens per batch
** E'_b determined for one prism per batch